



A NEW GEOTECHNICAL DATABASE FOR DYNAMIC SOIL PROPERTIES

*Considering Resonant Column and Cyclic
Triaxial Tests performed in France*

Work Package WP4

"Increasing the reliability of degradation curves for engineering uses"



AUTHORS		REVIEW		APPROVAL	
Name	Date	Name	Date	Name	Date
Samir BEDR Nathalie DUFOUR Emmanuel JAVELAUD Luca LENTI Julie REGNIER Cyril SIMON	2021/12/13	Dr PECKER A. Pr KAWASE H. 	2022/02/17 2022/08/04	 Emmanuel Viallet Public access <input checked="" type="radio"/> SIGMA-2 restricted <input type="radio"/>	2023-02-15

	Research and Development Program On Seismic Ground Motion	SIGMA2-2021-D4-083
		Page 2/50

DOCUMENT HISTORY

DATE	VERSION	COMMENTS
2021/12/13	1	<i>Submitted to official reviewers /waiting for suggestions</i>
2022/03/01	2	<i>Reviewed report with Dr. Alain Pecker's suggestions</i>

	Research and Development Program On Seismic Ground Motion	SIGMA2-2021-D4-083 Page 3/50
---	--	---------------------------------

EXECUTIVE SUMMARY

This report consists of 5 sections: (1) Introduction, (2) Review of International Databases for soil dynamic properties, (3) New geotechnical database of soil dynamic properties, (4) Comparisons with International Databases and (5) Conclusions. An appendix belonging to this document represents results of dynamic properties by range of confining pressure. The database is attached to this document in form of 3 files (an access file named SIGMA2-WP4.accdb, and 2 files excel named CTRP.xlsx, RESP.xlsx).

ABSTRACT & KEY WORDS

Dynamic soil properties are key parameters for seismic site analysis. These properties can be expressed in terms of variation of normalized equivalent shear modulus (G_{eq}/G_0), damping ratio (D) and normalized excess pore water pressure ($\Delta u/p'$) with the single amplitude shear strain (γ_{SA}). These properties can be measured using laboratory tests or in situ tests. These tests, which are expensive and difficult to perform, are often archived in different formats that do not facilitate their use and interpretation for further analysis.

This report presents the work accomplished in the framework of SIGMA2 project by EDF and Cerema, devoted to collecting French experimental data from Resonant Column (RC) and cyclic triaxial tests (CTX) performed by EDF and Cerema over the last 40 years. It accompanies the collection of the collected data that were homogeneously grouped and structured in a database useful to: 1) provide future statistical analysis on the variability of the physical variables describing the soils tested and of the results obtained, 2) establish correlations among relevant parameters, 3) deduce analytical predictions equations and 4) compare between analytical predictions related to other databases already published in literature.

In total, 240 specimens were collected, 59 from resonant column tests and 181 from cyclic triaxial tests coming from 21 sites. In comparison with three international geotechnical databases (Darendeli, 2001), (Zhang et al., 2005) and (Ciancimino et al., 2020a), the new here-proposed database represents the largest one in terms of number of specimens. Besides, the here-proposed database has three main particularities containing: 1) measurements of dynamic soil properties at very high mean effective confining pressure (up to 1600 kPa), 2) measurements of alluvial (sand/gravel) soils with particle size for which specific material and devices had to be considered and 3) measurements of pore water pressures with modulus and damping ratio.

The level of completeness of the here-proposed database and the possibility to use it jointly with other already-existing databases, open plenty of perspectives concerning the definition of the G_{eq}/G_0 , D and $\Delta u/p'$ curves as function of γ_{SA} . Next steps of the work will be dedicated to further analysis devoted to the quantification of the uncertainties affecting the dynamic soil properties.

Keywords: Database, modulus reduction curves, damping ratio, pore water pressure, shear strain, soil, resonant column test, cyclic triaxial test.

CONTENT

DOCUMENT HISTORY	2
EXECUTIVE SUMMARY	3
ABSTRACT & KEY WORDS	4
CONTENT	5
LIST OF FIGURES AND TABLES.....	6
LIST OF SYMBOLS AND ABBREVIATIONS	8
1 INTRODUCTION.....	9
1.1 SEISMO-TECTONIC CONTEXT OF FRANCE	11
1.2 SEISMIC GROUND MOTIONS AND SITE EFFECTS ESTIMATION.....	13
1.3 DYNAMIC SOIL PROPERTIES.....	15
1.4 PROBLEMATICS AND OBJECTIVES.....	19
2 REVIEW OF INTERNATIONAL DATABASES	20
3 FRENCH DYNAMIC SOIL PROPERTIES DATABASE.....	23
3.1 DATA PRESENTATIONS	23
3.2 RELATIONAL DATABASE	23
3.3 DATA INTEGRATION.....	27
3.4 PRELIMINARY ANALYSIS OF THE DATABASE	27
3.4.1 Cyclic Triaxial tests	28
3.4.1.1 Dynamic properties	29
3.4.1.2 Cross-correlations	31
3.4.1.3 Volumetric strain threshold.....	33
3.4.2 Resonant Column tests	33
3.4.2.1 Dynamic properties	33
3.4.2.2 Cross-correlations	36
4 COMPARISON WITH INTERNATIONAL DATABASES	38
5 CONCLUSIONS.....	41
REFERENCES	42
APPENDIX : DYNAMIC SOIL PROPERTIES BY RANGE OF CONFINING PRESSURE 45	
CYCLIC TRIAXIAL TESTS.....	45
RESONANT COLUMN TESTS	47

LIST OF FIGURES AND TABLES

LIST OF FIGURES

Figure 1 Normalized equivalent shear modulus reduction curves and definition of single amplitude strain ranges for laboratory tests reliability (from Arkinsos & Salfors, 1991; Mair & UNWIN, 1993).....	9
Figure 2 Zoning of seismic hazard in France (source BRGM website).....	12
Figure 3 (a) Contribution of different factors to the seismic motion at the free surface (after Kramer, 1996) ; (b) qualitative stratigraphic formation as responsible of site effects ; (c) qualitative dynamic curves obtained for soils under cyclic solicitations as function of the single amplitude shear strain (γ_{SA}) : variation of the normalized equivalent shear modulus (G_{eq}/G_0), damping ratio (D), normalized excess pore water pressure ($\Delta u/p'$)	14
Figure 4 Qualitative examples of engineering issues for which the cyclic soil behavior is considered for a reliable prediction of induced effects on soils and/or on structure : (a) Vehicle, (b) Train, (c) Crane rails, (d) Machine foundation, (e) Compaction, (f) Lock, (g) Tank or silo, (h) Offshore wind turbine, (i) Onshore wind turbine, (j) Earthquake.....	15
Figure 5 Approaches for measurement of dynamic properties of soils by the use of I) laboratory tests on core or reconstituted samples (CTX, RC, etc.) and on physical models (shaking tables, centrifuge devices, etc.) and II) by the use of in situ invasive testing (CPT, SPT) or geophysical prospection based on recordings of vibrations and earthquakes at the free surface (H/V, MASW, etc.).....	16
Figure 6 Examples of laboratory tests on samples and physical models: (a) Triaxial (b) True triaxial (c) Torsion on hollow cylinder (d) Simple shear (e) Direct shear (f) Vibrating table (g) Resonant column (h) Wave propagation measurement	16
Figure 7 Typical results of cyclic tests: (a) Resonant curve from RC tests where I and I_0 are respectively the area polar moment of inertia of the specimen and the mass polar moment of inertia of the driving system, H and ρ are respectively the height and mass density of the specimen, (b) Example of strain-stress path obtained during a cyclic triaxial test.....	17
Figure 8 Qualitative representation of reduction curves as functions of the distortion (reduction of normalized shear stiffness, G_{eq}/G_0 , increasing of damping D and increasing normalized pore water pressure $\Delta u/p'$).....	18
Figure 9 Influence of testing and geotechnical parameters on dynamic soil properties	22
Figure 10 Map showing the locations of the investigated sites (EDF blue, CEREMA orange).....	23
Figure 11 Data Format Schema (Group Hierarchy)	24
Figure 12 Repartition of the data according to (a) the type of tests (b) the soil type, (c) the Plasticity Index and (d) the mean effective confining pressure	28
Figure 13 Cyclic triaxial tests: respectively variation of equivalent axial modulus, damping and pore water pressure with single amplitude axial strain according to the soil type (a, b and c)	29
Figure 14 Cyclic triaxial tests: variation of equivalent axial modulus, damping ratio and pore water pressure with single amplitude axial strain according to mean effective confining pressure (a, b, c), to plasticity index (d, e, f) and number of cycle (g, h, i).....	30
Figure 15 Correlations between ε_{SA} , E_{eq} , D , u , p' , PI for the cyclic triaxial tests. The values are given for single amplitude axial strain between 0.0001 till 0.01%.....	31
Figure 16 Correlations between ε_{SA} , E_{eq} , D , u , p' , PI for the cyclic triaxial tests. The values are given for single amplitude axial strain between 0.01 till 0.1%.....	32
Figure 17 Correlations between ε_{SA} , E_{eq} , D , u , p' , PI for the cyclic triaxial tests. The values are given for single amplitude axial strain between 0.1 till 1%.....	32
Figure 18 Volumetric strain threshold against the confining pressure. The color scale refers to the number of cycles of loading.....	33
Figure 19 Resonant column tests; variation of equivalent shear modulus, damping and pore water pressure with single amplitude shear strain according to the soil type (a, b and c).....	34
Figure 20 Resonant column tests; variation of evolution of the three main dynamic soil properties: shear modulus curves (G_{eq}), damping ratio (D) and pore pressure (u) curves with single amplitude shear strain (γ_{SA}) according to the confining pressure (a, b and c) and according to the plasticity index (d, e and f)	35

Figure 21 Correlations between γ_{SA} , G_{eq} , D , p' , PI for the resonant column tests. The values are given for single amplitude shear strain between 0.0001 till 0.01 %	36
Figure 22 Correlations between γ_{SA} , G_{eq} , D , p' , PI for the resonant column tests. The values are given for single amplitude shear strain between 0.01 till 0.1 %	37
Figure 23 Correlations between γ_{SA} , G_{eq} , D , p' , PI for the resonant column tests. The values are given for single amplitude shear strain between 0.1 till 1 %	37
Figure 24 Comparison and discussion of the database proposed with the ones by Darendeli (2001) Zhang et al. (2008) and Cincimino et al. (2020) : (a) Sites/Locations, (b) Tests type, (c) Soil types, (d) PI (%), (e) Mean effective confining pressure, p' (kPa)	39
Figure 25 Cyclic triaxial tests; Young modulus curves versus the axial strain according to the soil type for different confining pressure ranges and for a number of cycles $N=5$ (a, b, c and d), according to the Plasticity Index for different confining pressure ranges and for a number of cycles $N=5$ (e, f, g and h), and according to the number of cycles for different confining pressure ranges (i, j, k and l)	45
Figure 26 Cyclic triaxial tests: evolution of the Damping curves with axial strain according to the soil type for different confining pressure ranges and for a number of cycles $N=5$ (a, b, c and d) according to the Plasticity Index for different confining pressure ranges and for a number of cycles $N=5$ (e, f, g and h) and according to the number of cycles for different confining pressure ranges (i, j, k and l)	46
Figure 27 Cyclic triaxial tests: evolution of the pore water pressure curves with axial strain according to the soil type for different confining pressure ranges and for a number of cycles $N=5$ (a, b, c and d) according to the Plasticity Index for different confining pressure ranges and for a number of cycles $N=5$ (e, f, g and h) and according to the number of cycles for different confining pressure ranges (i, j, k and l)	47
Figure 28 Resonant column tests; evolution of the shear modulus curves with distortion according to the soil type (a, b, c and d) and according to the Plasticity Index for different confining pressure ranges (e, f, g and h)	48
Figure 29 Resonant column tests; evolution of the shear modulus curves with distortion according to the soil type (a, b, c and d) and according to the Plasticity Index (e, f, g and h) and for different confining pressure ranges	49
Figure 30 Resonant column tests; evolution of the pore water pressure curves with distortion according to the soil type (a, b, c and d) and according to the Plasticity Index (e, f, g and h) and for different confining pressure ranges	50

LIST OF TABLES

Table 1 Dynamic soil properties literature review	21
Table 2 Groups	24
Table 3 Headings	25

LIST OF SYMBOLS AND ABBREVIATIONS

G_0	Maximal shear modulus	γ_{SA}	Single Amplitude shear strain
G_{eq}	Equivalent shear modulus	γ_{DA}	Double Amplitude shear strain
G_{eq}/G_0	Normalised equivalent shear modulus	γ_{dt}	Cyclic degradation shear strain threshold
I_0	Polar mass moment inertia loading system	γ_{lt}	Linear shear strain threshold
I_p	Plasticity Index	γ_{pt}	Pore water pressure shear strain threshold
V_s	Shear wave velocity	γ_{rt}	Rupture shear strain threshold
W_D	Dissipated energy in one cycle	γ_{vt}	Volumetric shear strain threshold
<i>DSDSS</i>	Double Specimen Direct Simple Shear test	ε_{DA}	Double amplitude axial strain
W_S	Stored energy in one cycle	ε_{SA}	Single amplitude axial strain
E_{eq}	Equivalent axial modulus	ε_{SA}	Single amplitude axial strain
p'	Mean effective confining pressure	θ_{max}	Vibration amplitude
f_0	Fundamental resonant frequency (Torsion)	σ'_m	Effective mean confining stress
<i>CTX</i>	Cyclic Triaxial test	σ'_v	Vertical effective stress
<i>RC</i>	Resonant Column	ω_0	Torsional resonance frequency
<i>TS</i>	Shear Torsion	Δu	Excess pore water pressure
D	Damping ratio	$\Delta u/p'$	Normalised excess pore water pressure
N	Number of loading cycles	θ	Torsional angle amplitude
<i>OCR</i>	Over Consolidation Ratio	ν	Poisson's coefficient
R	Specimen radius	ρ	Density
f_1 and f_2	Frequencies at which the amplitude is $\sqrt{2}/2$ times the amplitude of the resonance frequency f_0		
f	Loading frequency		
g	Gravity constant		
q	Deviatoric Stress		
u	Pore water pressure		

1 INTRODUCTION

The knowledge of the monotonic and cyclic behavior of soils is primordial to perform the design of new structures as well as for evaluating the already-existing structures' vulnerability in relation to the geological, mechanical, geotechnical and stratigraphic properties of the building sites. The degree of knowledge of the soil behavior under monotonic and cyclic loads is highly influenced by the real possibility to perform tests in situ and in laboratory. Those tests are dedicated to evaluate the physical properties of the soil (density, porosity, void index, grain size distribution in relation to UGCS classification, Atterberg limits, etc.), their compressibility, their maximum strengths in drained or undrained conditions, the volume changes or the pore pressure variations induced, estimations of elastic moduli, seismic wave velocities and energy dissipation properties as function of the strain induced.

Dynamic properties of soils are generally deduced from laboratory tests (such as Resonant Column tests and Cyclic Triaxial tests) and expressed in terms of variation of normalized equivalent shear modulus (G_{eq}/G_0), damping ratio (D) and normalized pore water pressure ($\Delta u/p'$) with single amplitude shear strain (γ_{SA}). These properties and their associated uncertainties are required for nonlinear site response analysis, for soil structure interaction and even for geotechnical studies involving weak cyclic motions such as in retaining wall or wind turbine foundations. More in general, the description of dynamic properties as functions are deduced considering different laboratory tests reliable for different ranges of single amplitude shear strain induced in the specimen (see Figure 1).

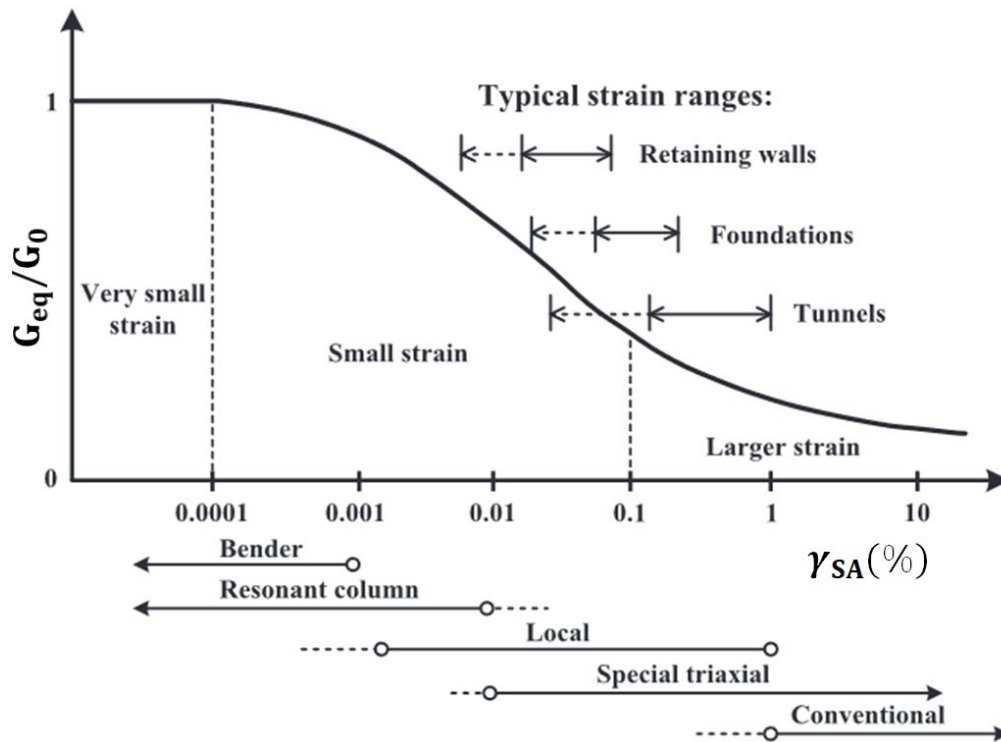


Figure 1 Normalized equivalent shear modulus reduction curves and definition of single amplitude strain ranges for laboratory tests reliability (from Arkinos & Sallfors, 1991; Mair & UNWIN, 1993)

The PRENOLIN project (2015-2021), put in evidence how it can be difficult to define these properties in a manner that could be useful for all the soil models tested during the numerical benchmark (Régner et al., 2018). Other difficulties concerning the current use of these dynamic properties are related to the fact that: 1) sometimes they are considered for sites different from the ones where they were cored on

	Research and Development Program On Seismic Ground Motion	SIGMA2-2021-D4-083
		Page 10/50

the basis of questionable hypothesis, 2) when available for the sites in study the curves describing the variables as function of the single shear strain amplitude can be affected by inherent uncertainties associated to the sample retrieving, specimen preparation, laboratory measurements, data interpretations and soil representativeness.

In recent years, attempts have been made to identify and quantify uncertainties related to the parameters required to the estimations of seismic hazard and seismic site effects. This was for instance the main objective of the SIGMA project. Nevertheless, the quantification and the reduction of uncertainties affecting the laboratory parameters describing the cyclic soil behavior remains a challenge. To this end, some databases concerning the parameters highlighting the non-linear soil behavior were produced in literature (Dobry & Vucetic, 1987; Vucetic & Dobry, 1991; Ishibashi & Zhang, 1993; Lanzo & Vucetic, 1999a; Darendeli, 2001; Hsu, 2002; Anderson, 2003; Menq, 2003; Zhang et al., 2005; Pyke et al., 2007; Matesic et al., 2010; Yoshida, 2015a; Kishida, 2017; Kumar et al., 2017; Dammala et al., 2019; Park & Kishida, 2019; Ciancimino et al., 2020a; Gobbi et al., 2020a; Facciorusso, 2021). In spite of these efforts, a database collecting the most part of the RC and CTX laboratory tests conducted on French soils was not elaborated up to now. In the framework of the WP4 of the SIGMA2 project, Cerema and EDF, worked on the definition of a geotechnical database devoted to collect all the experiment results obtained by EDF and Cerema (by the use of RC and CTX devices) from 1981 up to 2020 on cored samples.

The first goal of this document is to present the work done concerning the structuration of the geotechnical database and the preliminary homogenization of all available data (CTX and RC results) from EDF and Cerema laboratories. It was necessary to give a common format to all data by minimizing the discrepancies related to the different completeness of information available for each sample tested, and related to the different procedures adopted by various researchers and technicians during about 40 years depending on their experience. For this purpose, the database was created starting from the international format AGS (*Electronic Transfer of Geotechnical and Geoenvironmental Data AGS4*, 2020) as a reference and adding some of our own developments. The defined database contains data from 21 French sites; 59 specimens were tested at the RC and 181 at the CTX devices. The maximum amount of information for each site was achieved by considering all the documents available in different formats (digital files, paper reports, notes, etc.).

The second goal of the document is to make qualitative comparisons between the database produced during the SIGMA2 project and the ones already existing in literature in terms of completeness and limitations. It is worth saying that among all the databases on cyclic soil behavior presented in literature, only 3 were defined and used to make statistical analysis over data to deduce analytical formulations of the modulus, damping and pore water pressure curves depending on relevant parameters such as the soil type, the Plasticity Index (PI), mean effective confining pressures (p'), etc.

One of the perspectives of this current work is related to the use of this new provided database to find correlations among physical and state soil parameters and the above-mentioned curves. That work will allow the reduction of the uncertainties associated with the dynamic soil properties and will be useful to suggest French-specific analytical prediction equations for the non-linear functions (stiffness, damping and pore water pressure).

	Research and Development Program On Seismic Ground Motion	SIGMA2-2021-D4-083
		Page 11/50

1.1 SEISMO-TECTONIC CONTEXT OF FRANCE

Earthquakes are the most deadly natural hazard and cause the most damage. Between 2004 and 2011, earthquakes killed nearly 700 000 people worldwide. This phenomenon is one of the inevitable manifestations of plate tectonics, which exposes certain parts of the planet to a potential, permanent risk. Each year, about 100 000 earthquakes are recorded in the world. The most active seismic zones are located in Asia, Southern Europe, North Africa and America.

France, with the exception of the French indies, is a country with moderate seismicity. Metropolitan France and many territories (DOM-TOM, etc) are relatively far from the tectonic plate boundaries. Tectonic deformations in metropolitan France, mainly due to the collision of the Eurasian plate with the African one, are quite low (of the order of a millimeter per year), compared to other countries of the Mediterranean basin (i.e. magnitudes generally much lower than 6) and inhomogeneous on the territory. The most exposed regions are the mountain ranges of the Jura, Vosges, Alps and Pyrenees and in a less important manner, the Central Massif, the Armorican Massif, Provence and Corsica. A higher seismic risk is related to overseas French territories as illustrated in the seismic hazard map of France (see Figure 2).

In the French indies, seismicity is stronger, and the earthquakes are recognized as the first natural risk. Several destructive earthquakes have occurred there, notably that of January 11, 1839 (more than 300 deaths in Martinique) and that of February 8, 1843 (more than 3 000 deaths in Guadeloupe). French Polynesia is located in an intraplate zone and has low to moderate seismicity. New Caledonia is located in the vicinity of the New Hebrides subduction zone (the Australian plate plunges under the North Fijian basin), where there is intense seismic activity. Finally, the islands of Wallis and Futuna are located near the Tonga subduction zone and the Lau Basin where there is significant seismicity.

While the seismicity in mainland France is moderate, damaging events can occur. Those earthquakes can be close to cities such as Le Teil earthquake in 2019 having a magnitude Mw 4.2 (Ritz et al., 2020) or Annecy earthquake in 1993 with Mw 5.2, and more rarely larger events, for instance the Lambesc earthquake in 1909 with estimated magnitude Mw of 6.0 (Baroux et al., 2003) or the Ligurian earthquake in 1887 with estimated magnitude Mw between 6.8-6.9 (Larroque et al., 2012).

Each year, the French territory is subjected to about a hundred earthquakes with magnitude greater than 3 and about twenty with magnitude greater than 3.5, while several thousand are recorded in the entire Mediterranean basin. The seismic risk needs to be considered for current buildings and even more for critical facilities such as nuclear plants. The seismic ground motion has to be predicted with a high level of confidence. In low seismicity countries, observations of large earthquakes are not available; the predictions can be performed by extrapolating the observations of weak events or simulated using numerical approaches.

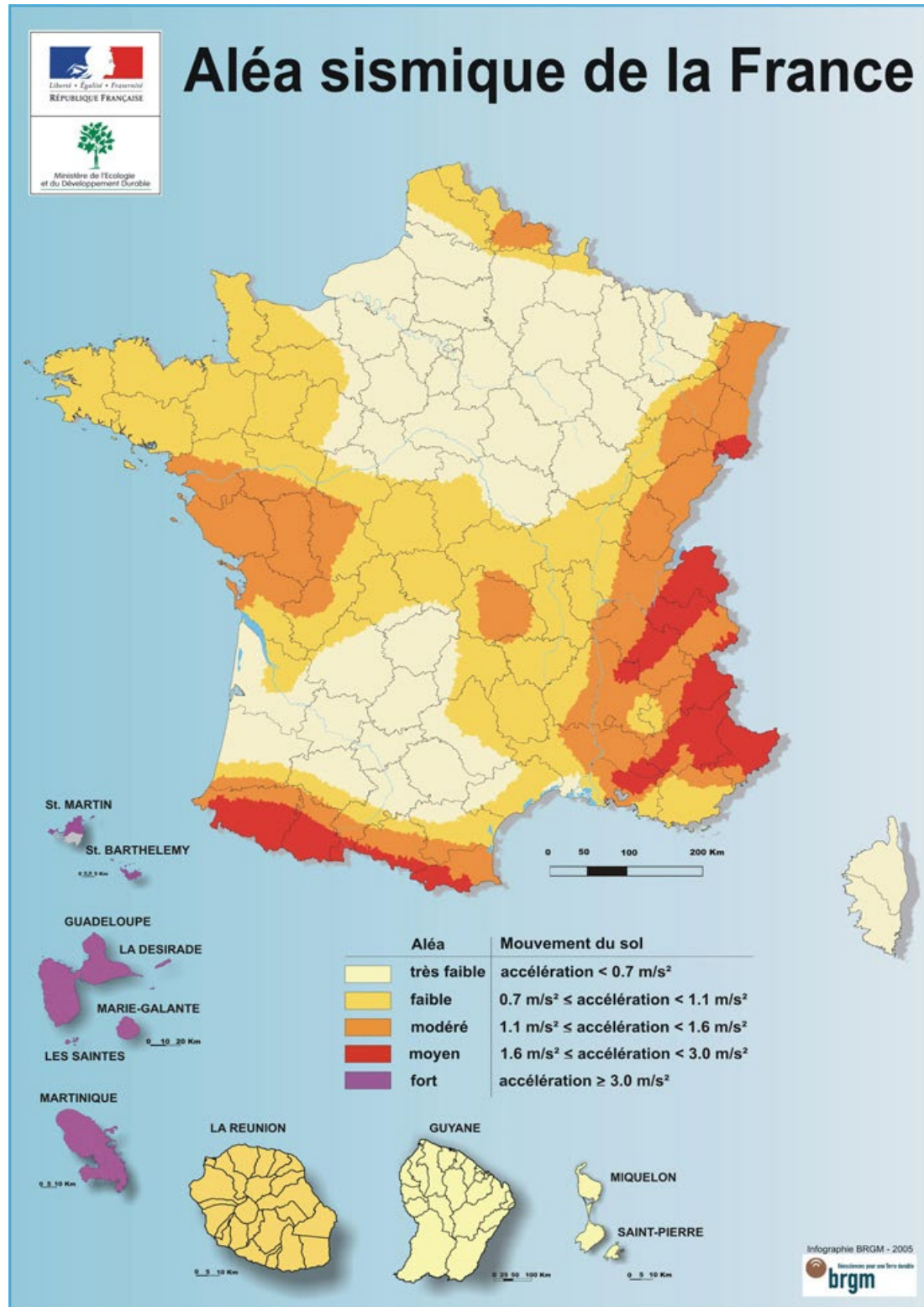


Figure 2 Zoning of seismic hazard in France (source BRGM website)

	Research and Development Program On Seismic Ground Motion	SIGMA2-2021-D4-083
		Page 13/50

1.2 SEISMIC GROUND MOTIONS AND SITE EFFECTS ESTIMATION

The seismic motion at the surface depends essentially on three factors (see Figure 3a), namely: 1) source effects, 2) path effects and 3) site effects. During an earthquake, a part of the energy of the process is released from the hypocenter in the form of seismic waves that travel in all directions. As they move away from the hypocenter, the waves will generally attenuate, so they should be less destructive with increasing distances. However, seismic observations have revealed site effects resulting in amplifications and frequency-dependent modulations of seismic motion at the surface (see Figure 3b). The propagation of the seismic waves through the subsurface soil layers can strongly modify locally the seismic motion recorded at the surface (Bard et al., 1988). Then the so-called site response depends on the geometrical configuration of the soil layers and on the mechanical behavior of the soils affected by the propagation (e.g. Bard & Bouchon, 1985; Figure 3b). During strong to moderate earthquakes, seismic wave propagation in the subsurface soft soil layers can induce large strains and trigger also a strong non-linearity in the soil behavior impacting significantly the site response (Régner et al., 2013). In the presence of undrained, saturated, poorly compacted and non-cohesive materials, the seismic solicitations can produce excess pore water pressure. If the water pore pressure reaches the overburden pressure, that leads to soil failure with the appearance of liquefaction phenomena (fluid liquefaction and mobility). In this situation, the soil no longer has the strength to support the stress thus large vertical and lateral permanent displacements can occur (Seed & Idriss, 1971).

The estimation of site effects can be performed empirically using recordings of ground motions recorded simultaneously at the studied site and at a reference site close by (i.e. located at the outcropping rock or in depth in the bedrock formation as in the case for downhole sensor configurations), or estimated with numerical simulations.

In this latter case to calculate the propagation of the seismic waves in a non-linear medium, most of the time, the soils are characterized by the normalized equivalent shear modulus reduction, increase of damping and increasing normalized pore water pressure curves and/or by the shear stress-strain hysteresis curves. In the PRENOLIN project (2015-2021), an international benchmark on 1-D non-linear site response estimation has been performed. One main highlight of the project was the difficulty to define a set of non-linear soil parameters that respect the requirements of the different codes in the benchmark, using at the same time in situ measurements, soil specimens and laboratory testing and/or generic curves from literature (Régner et al., 2018). When performing non-linear calculations, the engineers often use models based on the normalized equivalent shear modulus, damping and normalized pore water pressure curves. It is not rare they do not have data specific for the studied site, most of the time due to the high costs of its detailed geotechnical characterization; when data are available, the quality of the data can be questionable, because of the inherent uncertainties associated (sampling retrieving, specimen preparation, interpretation of the results and their representativeness in respect to geotechnical features of the site from which the sample was cored, etc.). The study of soil behaviour under cyclic loadings is largely carried out in the laboratory, by performing cyclic tests on soil specimens. These specimens are first saturated and consolidated to recreate the real and natural lithostatic conditions *in situ*, and then they are subjected to cyclic loadings to study their cyclic behaviour (Figure 3c).

Currently, studies of soil behavior under cyclic loadings are carried out using the dynamic properties of soils and considering the associated uncertainty curves; several authors have proposed models of uncertainty curves. The final purpose of the database that we defined working for the WP4 of SIGMA2 project is to quantify these uncertainties in a near future in the framework of the scientific partnership agreement between EDF and Cerema that will remain in force until the end of the project SIGMA2.

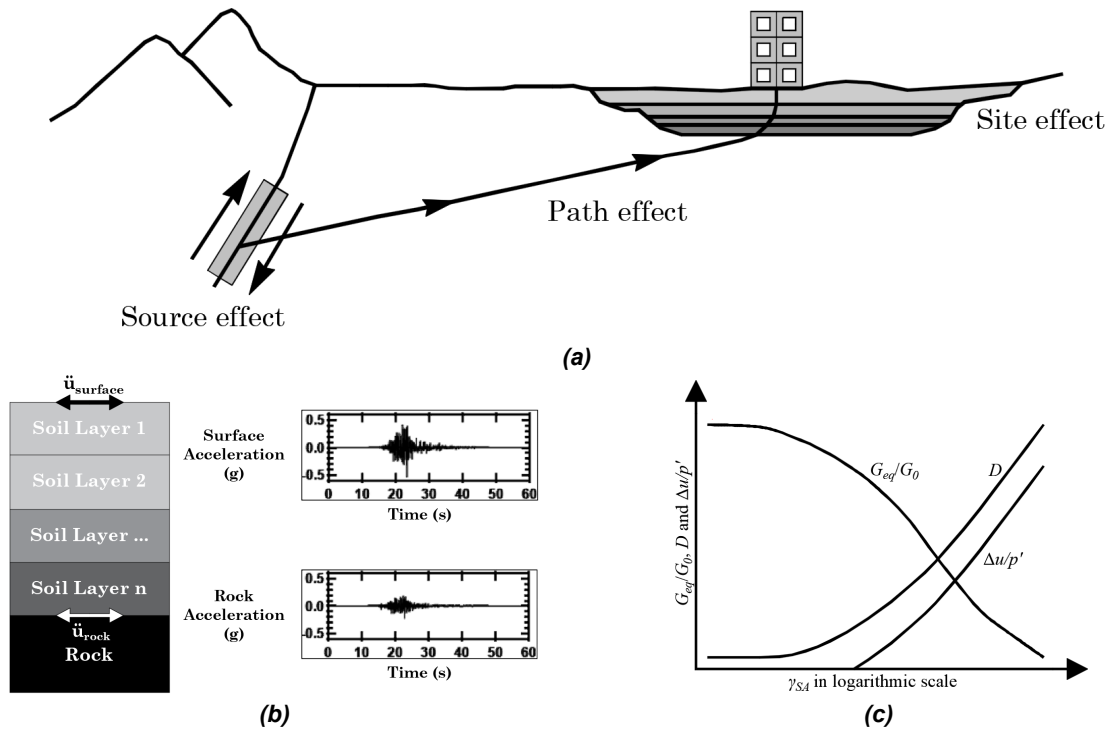


Figure 3 (a) Contribution of different factors to the seismic motion at the free surface (after Kramer, 1996) ; (b) qualitative stratigraphic formation as responsible of site effects ; (c) qualitative dynamic curves obtained for soils under cyclic solicitations as function of the single amplitude shear strain (γ_{SA}) : variation of the normalized equivalent shear modulus (G_{eq}/G_0), damping ratio (D), normalized excess pore water pressure ($\Delta u/p'$)

1.3 DYNAMIC SOIL PROPERTIES

Many geotechnical engineering problems are associated with cyclic loadings as illustrated in Figure 4. Cyclic loadings can be caused by anthropic sources such as traffic (vehicles, trains), industrial sources (crane rails, machine foundations), construction processes (vibration of sheet piles, etc.); repeated emptying and filling processes (locks, reservoirs, tanks and silos) or natural sources such as the wind, the waves (onshore and offshore wind turbines, coastal structures) and the earthquakes. The response of the soil under cyclic loading depends on the nature, the modalities of application of the cyclic loadings, and on the dynamic soil properties.

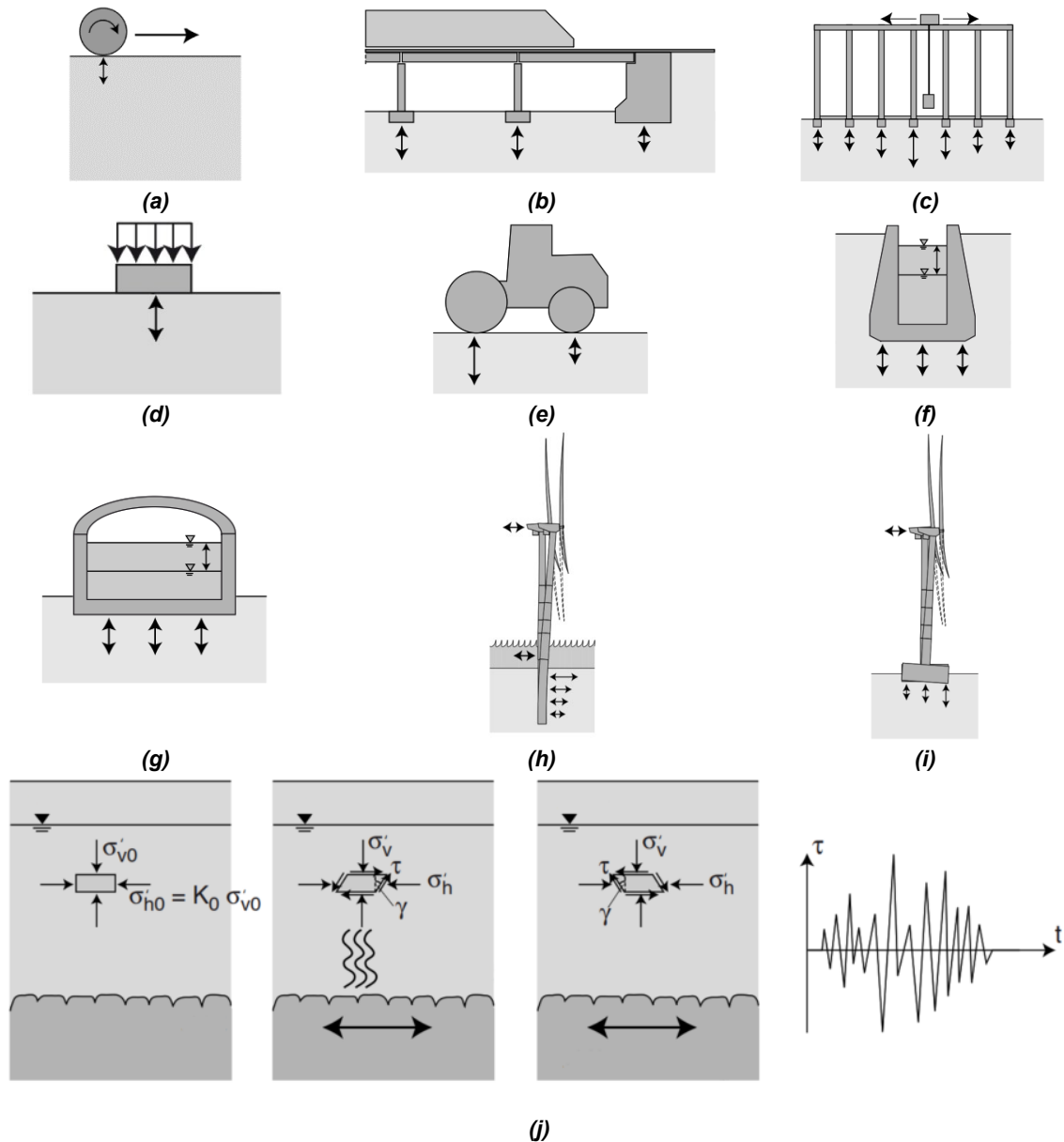


Figure 4 Qualitative examples of engineering issues for which the cyclic soil behavior is considered for a reliable prediction of induced effects on soils and/or on structure : (a) Vehicle, (b) Train, (c) Crane rails, (d) Machine foundation, (e) Compaction, (f) Lock, (g) Tank or silo, (h) Offshore wind turbine, (i) Onshore wind turbine, (j) Earthquake

Cyclic tests are expensive and difficult compared to other types of geotechnical laboratory tests, both in terms of implementation and interpretation. However, measurements of soil properties under cyclic loading conditions remain an essential task for solving most soil cyclic problems such as seismic site analysis, large area microzoning studies, and for geotechnical design in the cyclic domain (Pagliaroli, 2018). More in general, the measurement of dynamic soil properties can be performed by different methods, qualitatively reported on Figure 5.

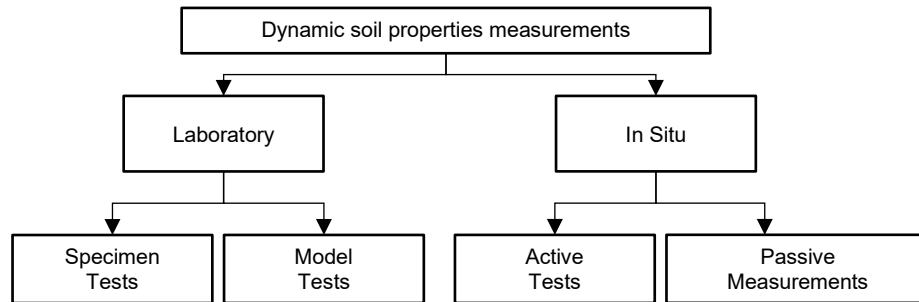


Figure 5 Approaches for measurement of dynamic properties of soils by the use of I) laboratory tests on core or reconstituted samples (CTX, RC, etc.) and on physical models (shaking tables, centrifuge devices, etc.) and II) by the use of in situ invasive testing (CPT, SPT) or geophysical prospection based on recordings of vibrations and earthquakes at the free surface (H/V, MASW, etc.)

The measurement of dynamic soil properties by in situ tests has the following advantages: 1) in situ testing does not require sampling (which can alter the stress, chemical, thermal, and structural conditions of the soil samples); 2) in situ testing measures the response of relatively large volumes of soil and 3) some experimental devices for in-situ prospections can induce large soil deformation as the attempts performed to extract dynamic soil properties by the means of the dynamic pressumeter (Mori & Tsuchiya, 1981). Measuring dynamic soil properties by laboratory tests also has many advantages: 1) laboratory tests allow to study the behavior of soils not only for the in situ assumed conditions but also for parametric studies (Figure 6); 2) laboratory tests allow drainage and the control of the excess of pore pressure generation and 3) laboratory tests provide a direct measurement of soil properties, unlike most in situ tests that determine them indirectly using empirical correlations.

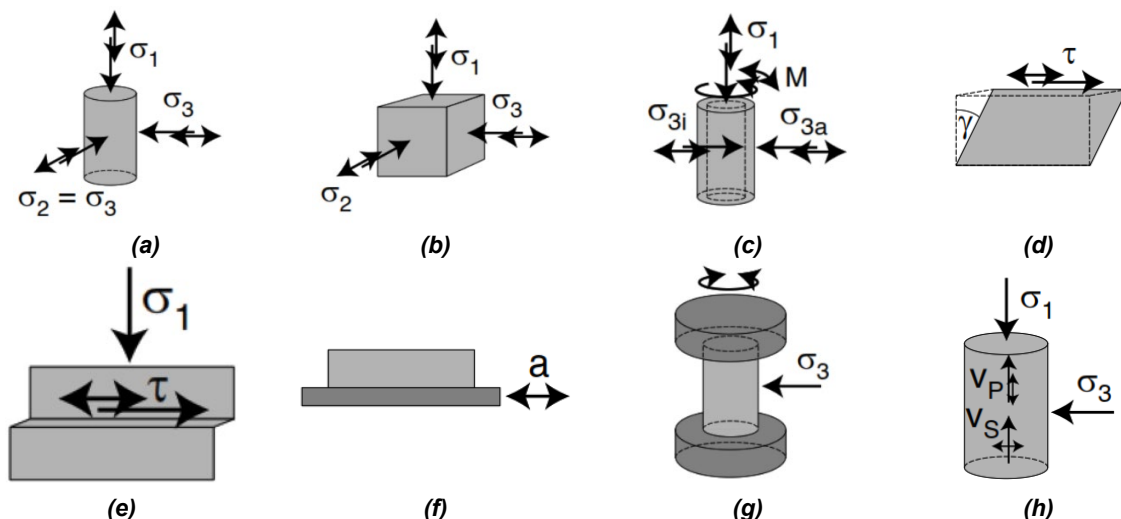


Figure 6 Examples of laboratory tests on samples and physical models: (a) Triaxial (b) True triaxial (c) Torsion on hollow cylinder (d) Simple shear (e) Direct shear (f) Vibrating table (g) Resonant column (h) Wave propagation measurement

Laboratory tests differ from one to each other depending on specimen boundary conditions (stress state, drainage, strain rate, etc.) and interpretation criteria. Among laboratory tests, those which are most used and standardized are the cyclic dynamic resonant column tests in resonance mode tests (*RC*) and the cyclic quasi-static triaxial tests (*CTX*).

The principle of *RC* tests is to vibrate a cylindrical specimen in torsional mode so that resonance condition can be established. A typical response curve deduced by the resonant column test is shown in the Figure 7(a). On Figure 7 is then reported the response in term of rotation induced at the top of the specimen acting with sinusoidal signals each at a given frequency and amplitude. Loading frequencies (f) greater than 20 Hz are generally applied and an accelerometer is used to monitor the movement of the specimen. The resonant frequency (f_0) and the maximum vibration amplitude associated (θ_{max}) are then determined from the response curve. The cyclic dynamic equilibrium at the resonance condition allows calculating shear wave velocity (V_s), G_{eq} and γ_{SA} by knowing the inertia of the loading device. Damping ratio (D) can be evaluated using the half-power bandwidth method by measuring the width of the frequency response curve around the resonance peak, specifically f_1 and f_2 which are the frequencies for which the amplitude is reduced by a factor of $\sqrt{2}$ respect to the maximum value θ_{max} .

In cyclic triaxial tests (*CTX*), the equivalent axial modulus (E_{eq}) is calculated from the slope of the line connecting the pick-to-pick hysteresis loop points as shown in Figure 7(b). Then, G_{eq} can be calculated by using the Poisson coefficient (ν). The damping ratio (D) is determined from the hysteresis loop as function of the ratio between the dissipated energy in a cycle (W_D) and the maximum elastic strain energy stored during the phase of first loading (W_S). The single shear strain (γ_{SA}) can also be calculated by using Poisson coefficient (ν).

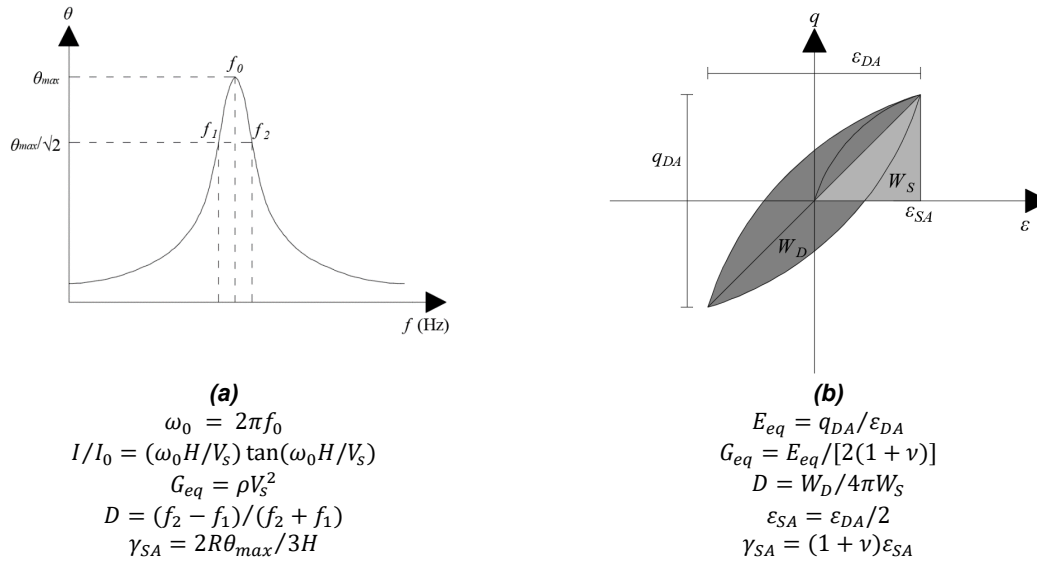


Figure 7 Typical results of cyclic tests: (a) Resonant curve from RC tests where I and I_0 are respectively the area polar moment of inertia of the specimen and the mass polar moment of inertia of the driving system, H and ρ are respectively the height and mass density of the specimen, (b) Example of strain-stress path obtained during a cyclic triaxial test

When the same test is conducted with increasing values of the imposed strain amplitudes, equivalent modulus, damping and pore water pressure curves can then be found as functions of the strain amplitude as reported on the Figure 8.

To describe the soil dynamic properties curves deduced from laboratory tests, Lo Presti & O'Neill (1991) introduced the concept of shear strain thresholds and Vucetic (1994) further clarified it (Figure 8). The

latter defines the linear shear strain threshold (γ_{lt}), below which soils behave linearly elastic (this term is used even though soils exhibit material damping at very low stresses when their cyclic behavior can be approximated by a viscoelastic constitutive model such Kelvin-Voigh, Maxwell body models and evolution of these last ones; Lenti (2017)) and the volumetric shear strain threshold (γ_{vt}) starting from which soils behave in a highly non-linear and hysteretic manner and undergo permanent changes in their microstructure. These microstructural changes are manifested by residual pore water pressure, decreased stiffness, and strength.

Between γ_{lt} and γ_{vt} , the soils exhibit non-linear elastic and hysteretic behavior, without significant microstructural changes. Tabata & Vucetic (2010) and Mortezaie & Vucetic (2016) distinguish the threshold for cyclic shear strain degradation (γ_{dt}) above which dynamic properties are also affected by the duration of the solicitation (i.e. in the laboratory from the number (N) of cycles imposed during CTX or RC tests) and degradation phenomena appear, and the threshold for shear strain pore pressure accumulation (γ_{pt}). It has been suggested (Vucetic, 1994) that these shear strain thresholds (γ_{dt} and γ_{pt}) are very similar as they are associated with the occurrence of permanent displacements between soil particles and subsequent irreversible rearrangement. More recently, Tabata and Vucetic (2010) and Mortezaie and Vucetic (2016) showed that γ_{dt} is typically smaller than γ_{pt} with a ratio (γ_{pt}/γ_{dt}) between 1.2 and 6.

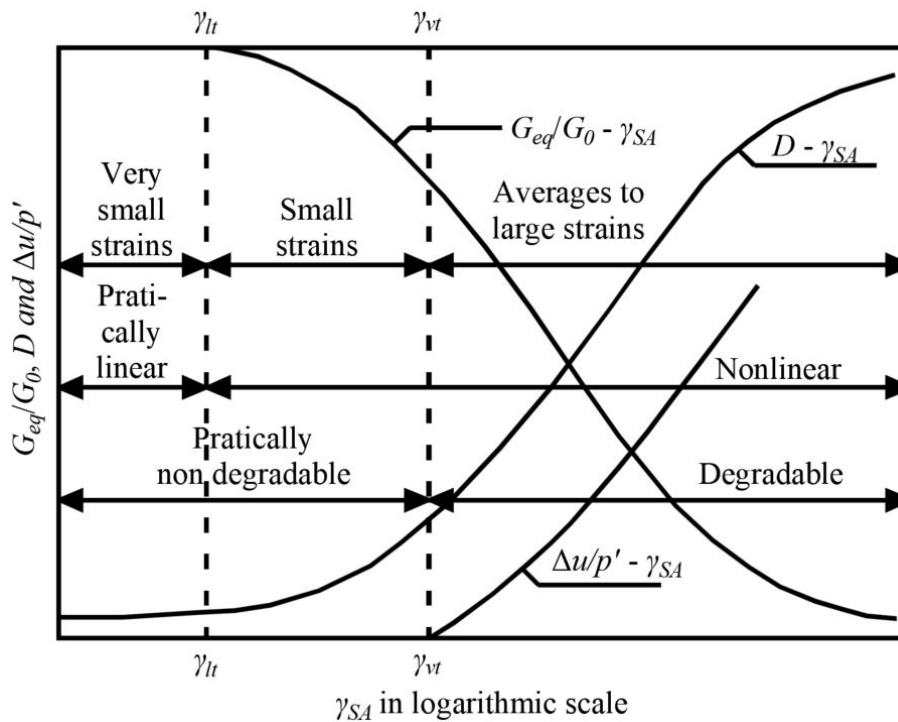


Figure 8 Qualitative representation of reduction curves as functions of the distortion (reduction of normalized shear stiffness, G_{eq}/G_0 , increasing of damping D and increasing normalized pore water pressure $\Delta u/p'$)

	Research and Development Program On Seismic Ground Motion	SIGMA2-2021-D4-083
		Page 19/50

1.4 PROBLEMATICS AND OBJECTIVES

To date, it is appropriate to make an effort to take into account all the studies carried out for the characterization of the behavior of French soils under cyclic loading since 1981. The studies are thus archived in different ways and in different laboratories. These tests, which are costly and difficult to perform, are often archived as: 1) unstructured data (images, photos, video, text or PDF); 2) semi-structured data (in XML, JSON, LOG etc.); and 3) structured data (in the form of tables of ASCII values, etc.)

The main objective of this work is to gather, digitize, structure and put in a standard format, all the reports concerning the soils which were the subject of dynamic properties measurements, having been made available by various national laboratories, by integrating, when available, also the results concerning their other geotechnical characterization/information.

The proposed database will be compared with other international databases, in order to see their respective advantages and shortcomings. Prospects will also be proposed for the use of this database for future research: completeness of the database, derivation of statistical correlations, prediction of the soil dynamic properties and associated uncertainties, impact of well-known properties such as the plasticity index and others (effective mean confining pressures, distributions of grain size, etc.) on the variability of the dynamic properties, review of literature concerning the uncertainties associated with natural variability of soils, of the variability depending on the quality of samplings and on the different procedures adopted in the laboratory.

2 REVIEW OF INTERNATIONAL DATABASES

17 papers from 1991 till today that published analysis of laboratory tests for characterizing the non-linear soil behavior are reviewed. The main scopes of these studies are to publish databases of structured data, to analyze the influence of state and physical parameters on the results obtained or to provide predictive models with associated uncertainties of dynamic parameters.

The synthesis of the papers is carried out according to the type of tested soils and performed tests, relevant parameters (tested or reviewed) and correlations deduced. Table 1 summarizes all this information.

Among the 17 papers reviewed, 3 focus on clay materials (Vucetic & Dobry, 1991; Zhang et al., 2005; Kishida, 2017), 4 on sands and gravels (Menq, 2003; Kumar et al., 2017; Dammala et al., 2019; Gobbi et al., 2020a; Hsu, 2002), 8 on clay and sands (Ishibashi & Zhang, 1993; Lanzo & Vucetic, 1999a; Darendeli, 2001; Anderson, 2003; Matesic et al., 2010; Ciancimino et al., 2020a; Facciorusso, 2021), 1 paper deals with clays earth core dam (Park & Kishida, 2019) and 1 paper provides an overview of cyclic behavior of Tuff rock (Pyke et al., 2007).

Five laboratory tests were performed: cyclic triaxial test (CTX), resonant column test (RC), torsional shear test (TS), Direct simple shear (DSS) and Double Specimen Direct Simple Shear (DSDSS).

Analytical relationships to describe the cyclic soil behaviour were derived from databases of laboratory tests, among the most used we can quote the relations provided by Dobry & Vucetic, (1987), Ishibashi & Zhang, (1993) or Darendeli, (2001) among others. The soil properties having the greatest influence on the cyclic soil behavior were retrieved.

Four main dynamic soil properties were analyzed in the papers, the maximum shear modulus (G_0), the normalized equivalent shear modulus reduction curve ($G_{eq}/G_0 - \gamma_{SA}$), the damping curves ($D - \gamma_{SA}$), and the low strain attenuation (D_{min}). The Authors investigated both the influence of geotechnical properties and testing parameters on the cyclic soil behaviour.

Among the studied geotechnical parameters, we can find: plasticity index (PI), mean effective confining pressure (p'), effective vertical stress (σ_v'), geological age (T_g), over consolidation ratio (OCR), degree of saturation (D_s), mean particle size (D_{50}), undrained shear strength (C_u), void ratio (e), relative density (D_r), fine content (f_c), while testing parameters are the soil/sample disturbance (SD), the loading frequency (F), the number of cycles (N) and the maximum strain (ϵ_{max}). Figure 9 indicates the influence of each state and parameter on dynamic soil properties reported in the literature. The influence is divided into 5 types: a change of a state and physical parameter that must cause an increase of the soil property (1); or it may cause an increase of the soil property (2); or it can have no influence on the soil property (3); or it may cause a decrease of the soil property (4); and finally it must cause a decrease of the soil property (5).

The analysis of this Figure 9 allows us to access the following observations:

- Maximum shear modulus (G_0): it increases with the effective confining pressure (reported by 3 papers). Vucetic & Dobry (1991) also reported an increase of G_0 with the frequency of loading, the OCR value and the geological age while an increase of the number of cycles and the void ratio decreases G_0 (also reported by Menq (2003)). According to Yoshida (2015) and Ciancimino et al., (2020), the disturbance of the soil decreases G_0 . Menq (2003) showed that an increase of D_{50} decreases G_0 . Finally, Gobbi et al., (2020) showed, on remoulded soil samples, that an increase of the relative density increases G_0 while the fine content decreases G_0 .

Table 1 Dynamic soil properties literature review

Databases	Number of specimens	Soil type	Tests					PR	Data Type	U E
			CTX	RC	TS	DSS	DSDSS			
Vucetic & Dobry, 1991	106	Clays	•	•		•		•	Document	
Ishibashi & Zhang, 1993		Sand and clays	•	•		•		•	Document	
Lanzo & Vucetic, 1999	81	Sand (22), clays (59)	•	•					Document	
Darendeli, 2001	110	Sand and clays		•	•			•	Document	•
Hsu & Vucetic, 2002	160	Sand and clays							Document	
Menq, 2003	59	Sand and Gravel		MMD			•		Document	
Anderson, 2003	40	Sand and Clays		25		15			Document	
Zhang et al., 2005	122	Clay		•		•		•	Document	•
Pyke et al., 2007	8	Non Welded tuff		22		22			Document	
Matesic et al., 2010	94	Sand and Clay				•			Document	
Kumar et al., 2017		Sand	•						Document	
Kishida, 2017	136	Clay and Silt							Document	
Dammala et al., 2019		Sand	•	•					Document	
Park & Kishida, 2019	31	Clays earth core dam		•					Document	
Gobbi et al., 2020	95	Silty Sand	56	39		•			Document	
Ciancimino et al., 2020	79	Silty and clayey	•	•		•	•	•	Document	•
Facciorusso, 2020	170	Sand and clay							Excel	

CTX: Cyclic triaxial
 RC: Resonant column
 TS: Torsional shear
 DSS: Direct simple shear
 DSDSS: Double specimen direct simple shear
 MMD : Multi Directional Device
 PR : Predictive Relations
 UE : Uncertainty Equations

- Normalized equivalent shear modulus (G_{eq}/G_0): most of the studies agree on the fact that the curves are mainly dependent on the mean confining pressure (p') and the plasticity index (PI) in a way that an increase of these parameters induced an increase of the curves, i. e. the soil behaviour tends to be more linear. Vucetic & Dobry (1991) indicated that the void ratio and two testing parameters (maximal deformation and the number of cycles) have also a great influence. The influence of the maximal deformation is also reported in Zhang et al. (2005) and Darendeli (2001). The influence of the vertical stress and the coefficient of uniformity is reported by only one study.
- Damping ratio (D): similarly to the shear modulus reduction curves, the mean confining pressure (p') and the Plasticity Index (PI) have the greatest influence on the damping curves. An influence of the vertical stress and void ratio is also proposed by only one study. Kumar et al. (2017) proposes to calculate the dynamic properties on asymmetrical stress-strain curves. The damping ratio can be 40% to 70% lower than the one obtained from symmetrical Hysteresis loops.
- Small strain damping ratio (D_{min}): Lanzo & Vucetic, (1999) published a work on the impact of the soil plasticity on small strain damping values. They indicated that the scatter of D_{min} is higher for soil with low PI values and that the damping ratio increases with PI .
- Yoshida (2015) and Ciancimino et al., (2020) show the influence of soil disturbance (SD) and damping processes by comparing in situ and laboratory measured shear modulus. In Yoshida (2015), the laboratory to in situ shear modulus ratio goes below one from 100 MPa and decreases when in situ shear modulus increases. Ishihara (1996) proposes correction factors to consider these effects. The corrections are greater for reconstituted samples. In Ciancimino et al., (2020) the laboratory to in situ V_s ratio goes below one from in situ shear wave velocity of 300 m/s.

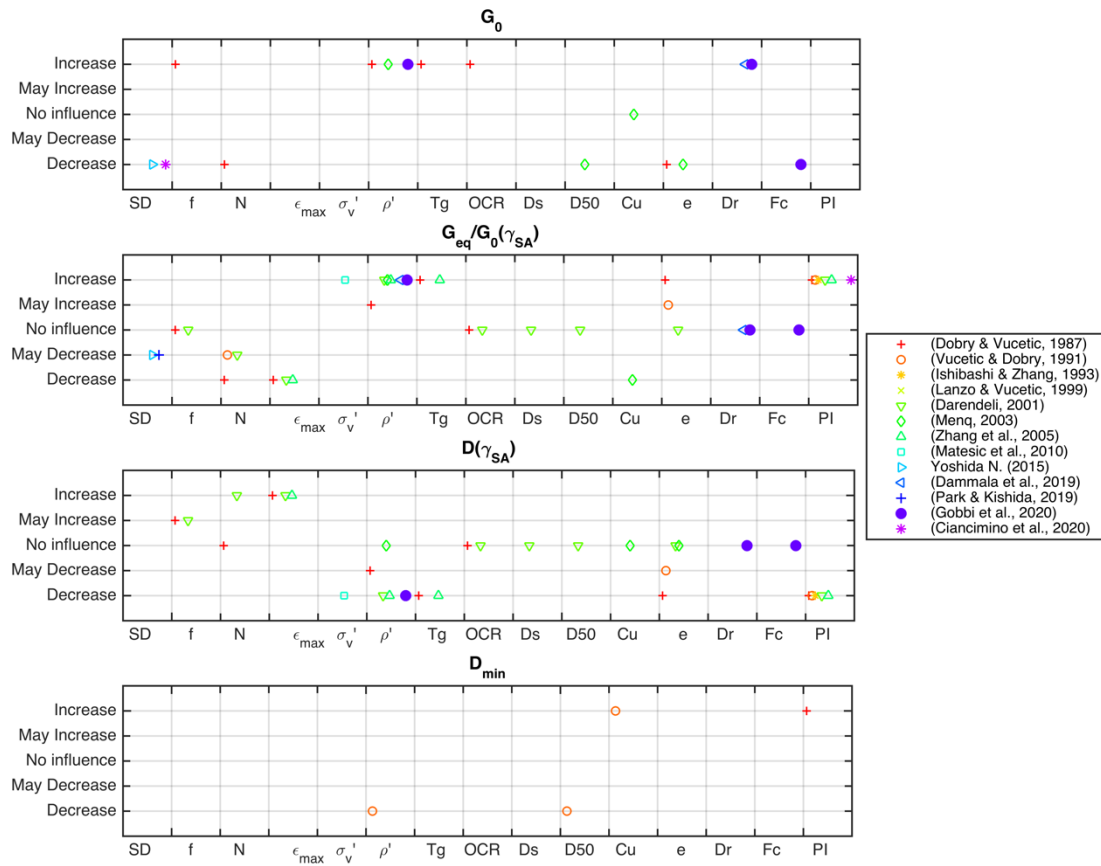


Figure 9 Influence of testing and geotechnical parameters on dynamic soil properties

3 FRENCH DYNAMIC SOIL PROPERTIES DATABASE

3.1 DATA PRESENTATIONS

Data were provided by two institutions, CEREMA and EDF. Data concerning investigations conducted for 21 sites from 1981 to 2020 were collected. Locations of the sites are presented in Figure 10.

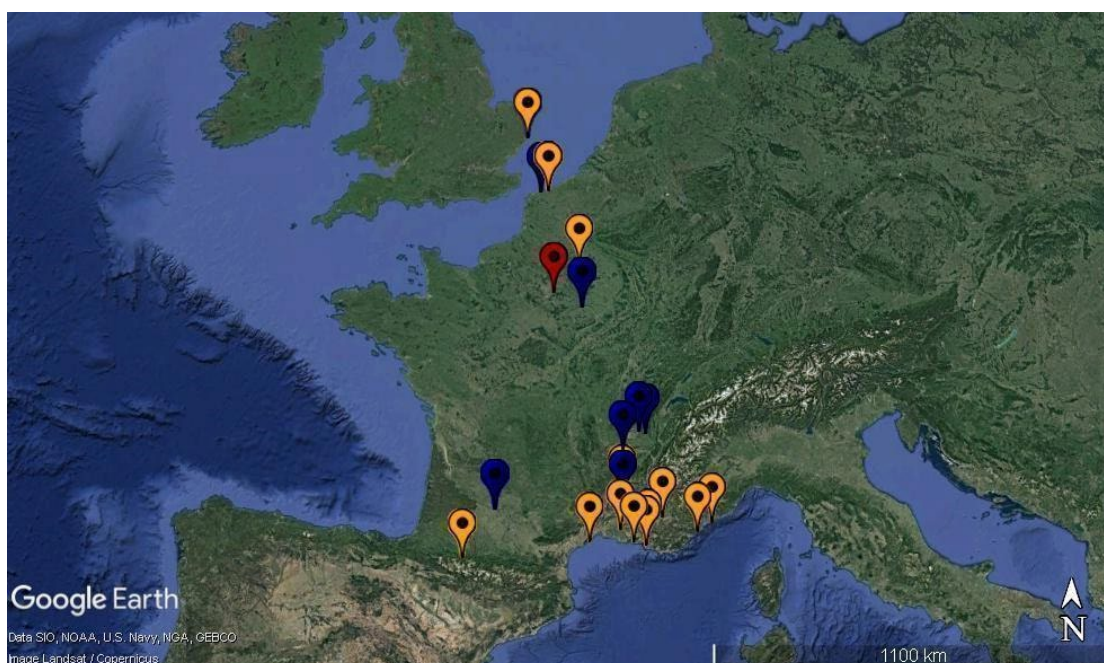


Figure 10 Map showing the locations of the investigated sites (EDF blue, CEREMA orange).
Map data: Google, SIO, NOAA, U.S. Navy, NGA, GEBCO

3.2 RELATIONAL DATABASE

The database has been developed by reproducing as faithfully as possible the AGS format (*Electronic Transfer of Geotechnical and Geoenviromental Data AGS4*, 2020). This format is under development by the Association of Geotechnical and Geoenviromental Specialists (AGS) and it is used by many geotechnical practitioners as being appropriate for electronic data transfer and storage. The AGS format is a structured list of data items that may be recorded during geotechnical and geoenviromental investigations (including testing and monitoring).

Those items are organized into groups. Each group contains a list of data headings which contain individual data variables (types, units, descriptions). The groups are organized in a hierarchy (see Figure 11). One group has only one parent defined in the hierarchy, but there can be many child groups below each parent. Each child group is linked to its parent group by identifier fields. The Table 2 defines the group hierarchy of our database by indicating the parent for each group. Actually, there are 15 groups in our database: prov, PROJ, LOCA, SAMP, CRTG, CRTC, crtq, CRTP, RESG, RESC, resq, RESP, LLPL, GRAG and GRAT. The Table 3 defines the heading of each one.

For our database, we needed to make some changes to take care of different aspects of collected data. We adopted the trick that abbreviations written in uppercase (example: PROJ) were already defined in the AGS format, and the ones written in lower case (example: prov) were added by ourselves. These propositions/changes can be, thereafter, proposed to the association of geotechnical and geoenvironmental specialist (AGS) as useful for their adoption.

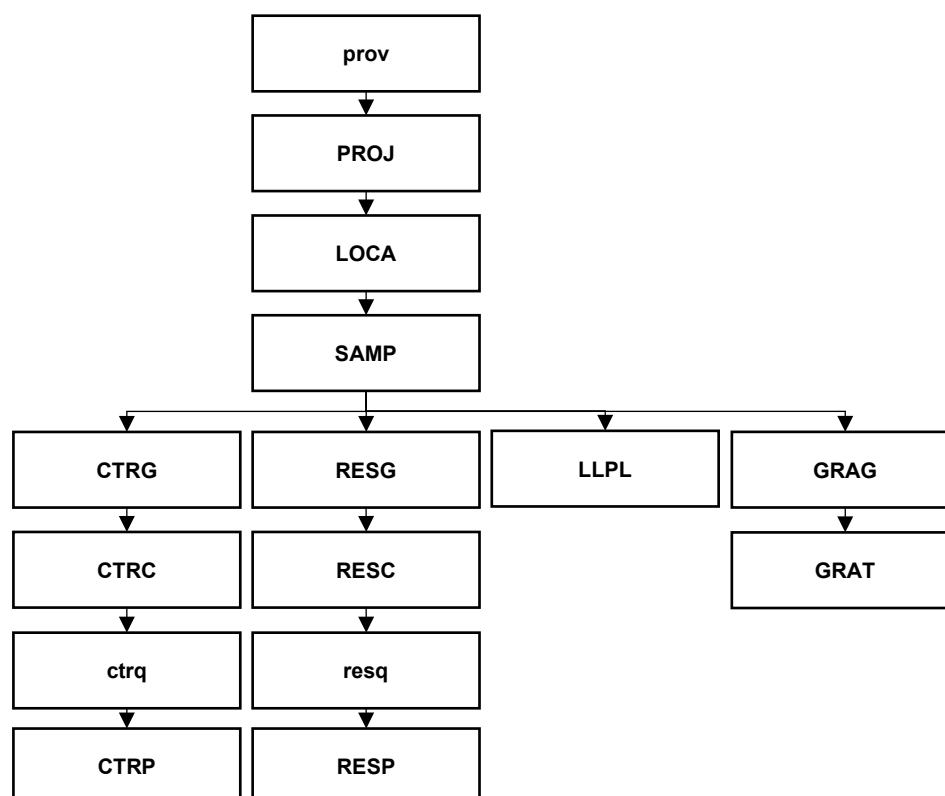


Figure 11 Data Format Schema (Group Hierarchy)

Table 2 Groups

Group Name	Contents	Parent Group
prov	Provider information	-
PROJ	Project information	prov
LOCA	Location Details	PROJ
SAMP	Sample Information	LOCA
CTRG	Cyclic Triaxial Test - General	SAMP
CRTC	Cyclic Triaxial Tests - Consolidation	CTRG
crtq	Cyclic Triaxial Tests - Sequence	CRTC
CRTP	Cyclic Triaxial Test - Derived Parameters	crtq
RESG	Resonant Column Test – General	SAMP
RESC	Resonant Column Test - Consolidation	RESG
resq	Resonant Column Test - Sequence	RESC
RESP	Resonant Column Test - Derived Parameters	resq
LLPL	Liquid and Plastic Limit Tests	SAMP
GRAG	Particle Size Distribution Analysis - General	SAMP
GRAT	Particle Size Distribution Analysis - Data	GRAG

Table 3 Headings

Group Name	Heading	Unit	Description
prov	prov_id	(-)	Provider identifier
	prov_name	(-)	Provider name
PROJ	PROJ_ID	(-)	Project identifier
	prov_id	(-)	Provider identifier
	PROJ_NAME	(-)	Project title
	proj_year	(-)	Project year
	PROJ_MEMO	(-)	General project comments
LOCA	LOCA_ID	(-)	Location identifier
	PROJ_ID	(-)	Project identifier
	loca_ref	(-)	Location reference
	loca_lat	(°)	Location latitude
	loca_lon	(°)	Location longitude
SAMP	SAMP_ID	(-)	Sample unique identifier
	LOCA_ID	(-)	Location identifier
	SAMP_REF	(-)	Specimen reference
	SAMP_TOP	(m)	Depth to top of sample
	SAMP_BASE	(m)	Depth to base of sample
	SAMP_DESC	(-)	Specimen description
	samp_type	(-)	Short sample descriptions
CTRG	CTRG_ID	(-)	Identifier
	SAMP_ID	(-)	Sample unique identifier
	SPEC_REF	(-)	Specimen reference
	spec_dpth	(m)	Depth of test specimen
	CTRG_SDIA	(mm)	Initial specimen diameter
	CTRG_HIGT	(-)	Initial height of specimen
	ctrq_cond	(-)	Sample condition
CTRC	CTRC_ID	(mm)	Identifier
	CTRG_ID	(-)	Cyclic Triaxial Test Consolidatin identifier
	CTRC_MNSE	(kPa)	Mean effective stress at the end of the stage
	ctrc_esecmax	(MPa)	Secant modulus max
	ctrc_smodmax	(MPa)	Shear modulus max
ctrq	ctrq_id	(-)	Sequence identifier
	CTRC_ID	(-)	Identifier
	ctrq_ordr	(-)	Sequence order
	ctrq_ref	(-)	Sequence reference
	ctrq_prcs	(1/0)	Sequence previously consolidated
CRTP	CTRP_ID	(-)	Identifier
	ctrq_id	(-)	Sequence identifier
	CTRP_CYC	(-)	Cycle number
	ctrp_qda	(kPa)	Duble amplitude deviatoric stress
	ctrp_eamsa	(%)	Single amplitude axial strain
	CTRP_ESEC	(MPa)	Secant modulus
	ctrp_damp	(%)	Damping ratio
	ctrp_pwp	(kPa)	Pore water pressure
RESG	RESG_ID	(-)	Identifier
	SAMP_ID	(-)	Sample unique identifier
	SPEC_REF	(-)	Specimen reference
	spec_dpth	(m)	Depth of test specimen
	RESG_SDIA	(mm)	Initial specimen diameter
	RESG_HIGT	(mm)	Initial height of specimen
	RESG_COND	(-)	Sample condition
RESC	RESC_ID	(-)	Identifier
	RESG_ID	(-)	Identifier
	RESC_MNES	(kPa)	Mean effective stress at the end of the stage
	resc_amodmax	(MPa)	Axial modulus max

Group Name	Heading	Unit	Description
	resc_smodmax	(MPa)	Shear modulus max
resq	resq_id	(-)	Identifier
	RESC_ID	(-)	Identifier
	resq_ordr	(-)	Sequence order
	resq_ref	(-)	Sequence reference
	resq_prcs	(1/0)	Sequence previously consolidated
RESP	RESP_ID	(-)	Identifier
	resq_id	(-)	Identifier
	resp_yamsa	(%)	Single amplitude shear strain
	resp_smod	(MPa)	Shear modulus
	RESP_DAMP	(%)	Damping
	resp_pwp	(kPa)	Pore water pressure
	resp_eamsa	(%)	Single amplitude axial strain
	resp_omod	(MPa)	Axial modulus
LLPL	LLPL_ID	(-)	Identifier
	SAMP_ID	(-)	Identifier
	LLPL_LL	(%)	Liquid limit
	LLPL_PL	(%)	Plastic limit
	llpl_pi	(%)	Plasticity Index
	llpl_ci	(-)	Consistence index
	llpl_li	(-)	Liquidity index
	llpl_ac	(-)	Activity
GRAG	GRAG_ID	(-)	Identifier
	SAMP_ID	(-)	Identifier
	SPEC_REF	(-)	Specimen reference
GRAT	GRAT_ID	(-)	Identifier
	GRAG_ID	(-)	Identifier
	GRAT_SIZE	(mm)	Sieve or particle size
	GRAT_PERP	(%)	Percentage passing/finer than GRAT_SIZE

	Research and Development Program On Seismic Ground Motion	SIGMA2-2021-D4-083
		Page 27/50

3.3 DATA INTEGRATION

The provided data had three different formats: 1) unstructured data (PDF, text, images, etc.); 2) semi-structured data (XML, JSON, LOG, etc.); and 3) structured data (tabular data, ASCII, etc.). The unstructured data (PDF, text, images, etc.) were digitalized using Webplotdigitizer, an online free code (Rohatgi, 2021). Python scripts are created and used to read from semi-structured (XML, JSON, LOG, etc.) and structured data files (tabular data) and then write them in the standard format into the database. The results of the particle size distribution analysis, Atterberg limit tests, cyclic triaxial tests and those of the resonant column have been successfully introduced. The results of other tests could be digitized/introduced in the future such as the shear or compressional wave velocity measured by bender elements tests, modulus and damping ratio measured by local strain measurements (LVDT or Hall effect sensors) during cyclic triaxial tests, the results of torsional shear tests or the 1D consolidation tests.

3.4 PRELIMINARY ANALYSIS OF THE DATABASE

The database contains tests performed on cored samples coming from 21 sites in France. In total 181 triaxial tests and more than 76 resonant columns tests are compiled (Figure 12-a). Among the 76 results from resonant column tests, only 59 consist of one test per specimen and the others 17 are second tests performed on the same specimen but with a different confining pressure.

For each cyclic triaxial test a value of equivalent axial modulus, damping ratio, pore water pressure and single amplitude axial strain are available for each number of cycles. The calculation of the axial modulus and damping from the hysteresis loop is challenging especially at high deformation when the shape of the curves can drastically change and even cannot close. In the Cerema reports, the procedure defined by (Serratrice, 2016) is proposed to identify the dynamic properties for cyclic triaxial testing. In this procedure, for each sequence of cycles controlled in strain mode, approximations of the recorded curves as a function of time are calculated in the sense of least squares methods by using Fourier series (Bessel approximations). For the other reports, the method is unknown. Among the 181 specimens tested with cyclic triaxial tests, the maximal axial modulus is available for 61. These values come from interpretation of the measurements and not direct measurements. While for the resonant column tests among the 59 specimens the maximal shear modulus measured is available for 46. This database contains only absolute axial and shear modulus reduction curves. Our next work will be to predict non-linear soil properties models. We propose to deduced normalized modulus reduction curves, damping ratio and pore water pressures functions from cyclic triaxial tests and Resonant columns tests.

In total the database is composed of 15 994 and 768 records for *CTX* and *RC* tests respectively. Among the specimens tested, 23 were performed on sand and gravel soils, 89 on clay and marl, 73 on sand, 4 on silt, 14 on mining residual and the geological description is not available on 37 specimens so-called undefined (Figure 12-b). The Plasticity Index (*PI*) is known on 72 specimens and undefined for the 168 specimens (Figure 12-c). The minimal *PI* value is 11% and the maximum reaches 90% with an average of 22%. This database has been built without any interpretation of the data. However, for the computation of predictive models additional data would be required. One way to increase the number of *PI* values would be to attribute a *PI* equal to 0% for sand specimens for instance, this can decrease the number of unknowns *PI* specimens value from 168 to 78. The database contains a large variability of confining pressure tested: 132 specimens were tested at a confining pressure below 400 kPa, 98 for a confining pressure between 400 and 800 kPa, 12 between 800 and 1200kPa and 4 specimens were tested at a confining pressure above 1200 kPa. The confining pressure is unknown for 11 specimens tested (Figure 12-d).

During our first analysis, we have observed that some properties exhibit outliers' values in the cyclic triaxial test results (2 values of axial modulus are < 0 MPa, 211 values of damping are $< 0.01\%$ and 6 values are $> 100\%$, 128 values of pore water pressure are < -29). The outliers' values are excluded. This selection is only performed on the two files accompanying this data base, namely CTRP.xlsx and RESP.xlsx and not in the original SIGMA2-WP4.accdb. All following figures and analysis consider the filtered data.

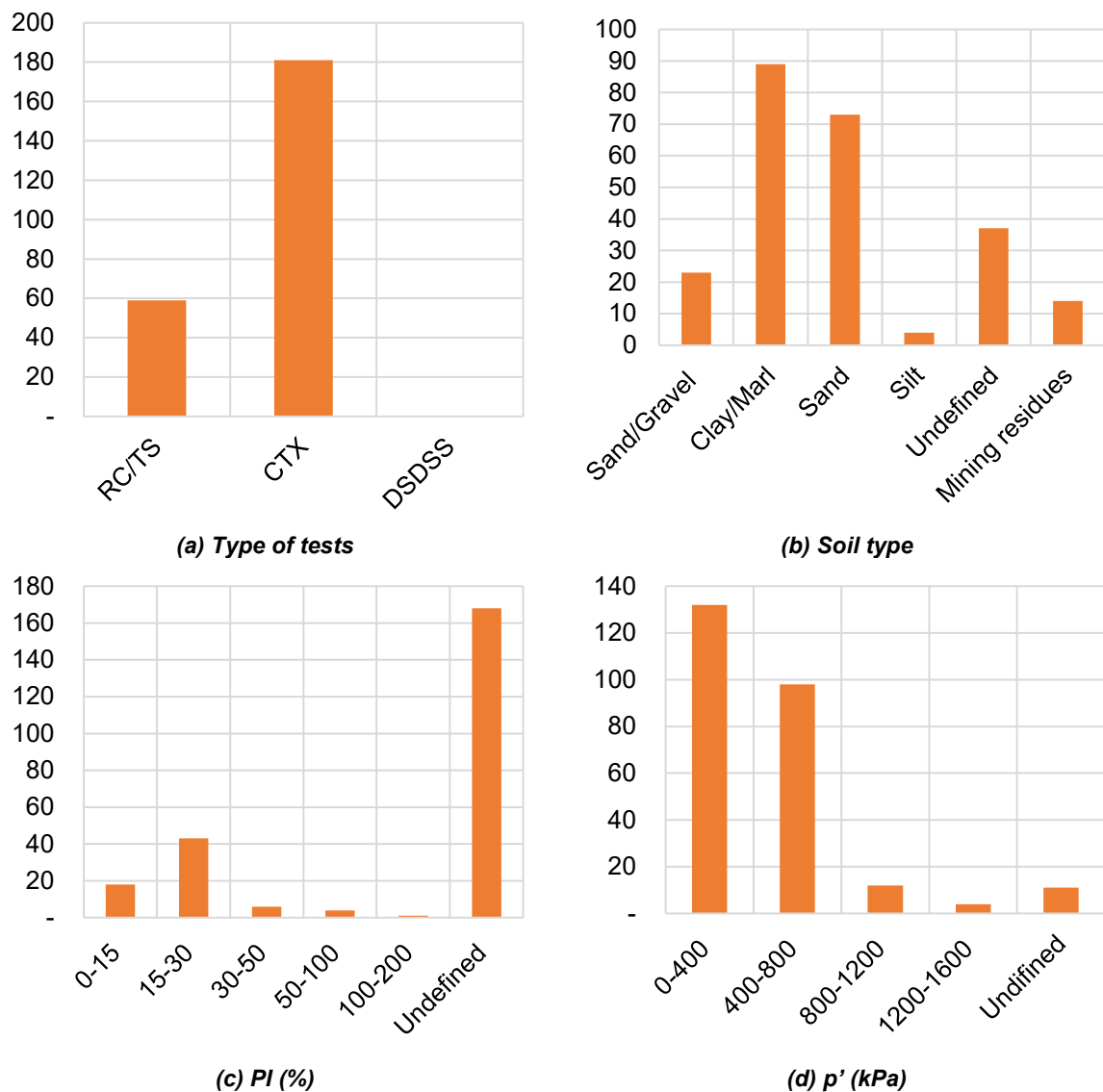


Figure 12 Repartition of the data according to (a) the type of tests (b) the soil type, (c) the Plasticity Index and (d) the mean effective confining pressure

3.4.1 Cyclic Triaxial tests

The following sections present : the evolution of the main dynamic soil properties, axial modulus, damping and pore water pressure according to the single-amplitude axial strain (ϵ_{SA}) for the cyclic triaxial tests, cross-correlations and distributions of pertinent parameters for three single-amplitude axial strain intervals and calculation of volumetric axial strain threshold. To illustrate the influence of two parameters simultaneously on the dynamic soil properties, results are stored according to the mean effective confining pressure and another physical/laboratory parameter (soil type, plasticity index, or number of cycles), figures and comments are presented Appendix.

3.4.1.1 Dynamic properties

The influence of the soil type is illustrated on the Figure 13. The largest equivalent axial modulus is obtained for sands and soils of sand and gravel. This study was performed on alluvium (sand/gravel) soils with specific material to handle large particle size. According to Figure 13b the damping ratio is larger for sand and gravel soils. In the previous graph we have seen that the pore water pressure increases with PI but it seems only true for clay materials indeed on Figure 13c while the pore water pressure shows similar trend for sand and clay materials.

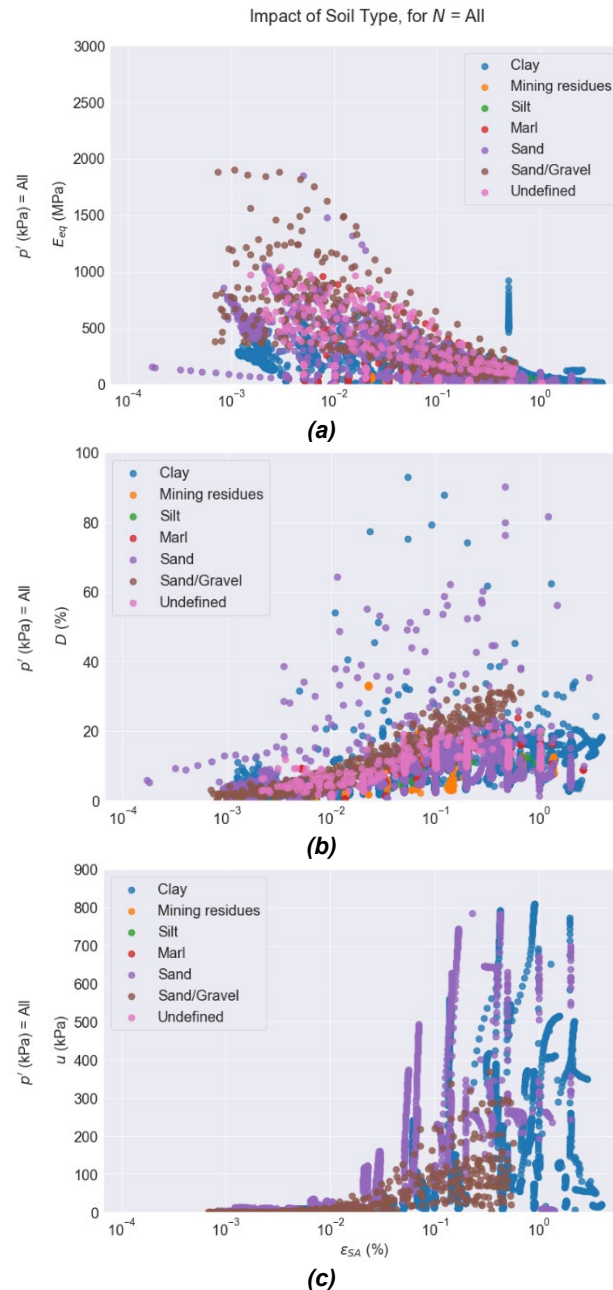


Figure 13 Cyclic triaxial tests: respectively variation of equivalent axial modulus, damping and pore water pressure with single amplitude axial strain according to the soil type (a, b and c)

The influence of the confining pressure is illustrated on the Figure 14 (a, b and c). We can observe that the minimal single amplitude axial strain is around $\varepsilon_{SA}=10^{-4}$ % and the maximum reaches $\varepsilon_{SA}=8\%$. The maximum value of the equivalent axial modulus reaches almost 2000 MPa for a confining pressure of 500 kPa. We would expect an increase of the equivalent axial modulus with the confining pressure (as mentioned by Dobry & Vucetic (1987), Menq (2003) and Gobbi et al (2020)) but there is no clear tendency on the figure. For the damping ratio, we can see that the maximal measured attenuation reaches 90 % (which seems to be a very high value) and has been observed in tests with effective confining pressure below 500 kPa. The damping seems to decrease with increasing confining pressure, but further quantitative investigations should be led to confirm this tendency. The pore water pressure appears to increase with increasing effective confining pressure reaching values of 800 kPa.

The influence of the plasticity index is illustrated on the Figure 14 (d, e and f). There is less data compared to the previous subgraphs and this is because PI is not always known for each test and it is not considered for sand materials. The plasticity index does not appear to have a large influence on the equivalent axial modulus and damping ratio. However, we can observe that the pore water pressure is larger at larger PI values.

The influence of the number of cycles on the dynamic properties is illustrated in the Figure 14 (g, h and i). When the number of cycles increases, we can observe the equivalent axial modulus and the damping ratio decrease (this has been also observed by Dobry & Vucetic (1987)) while the pore water pressure clearly increases.

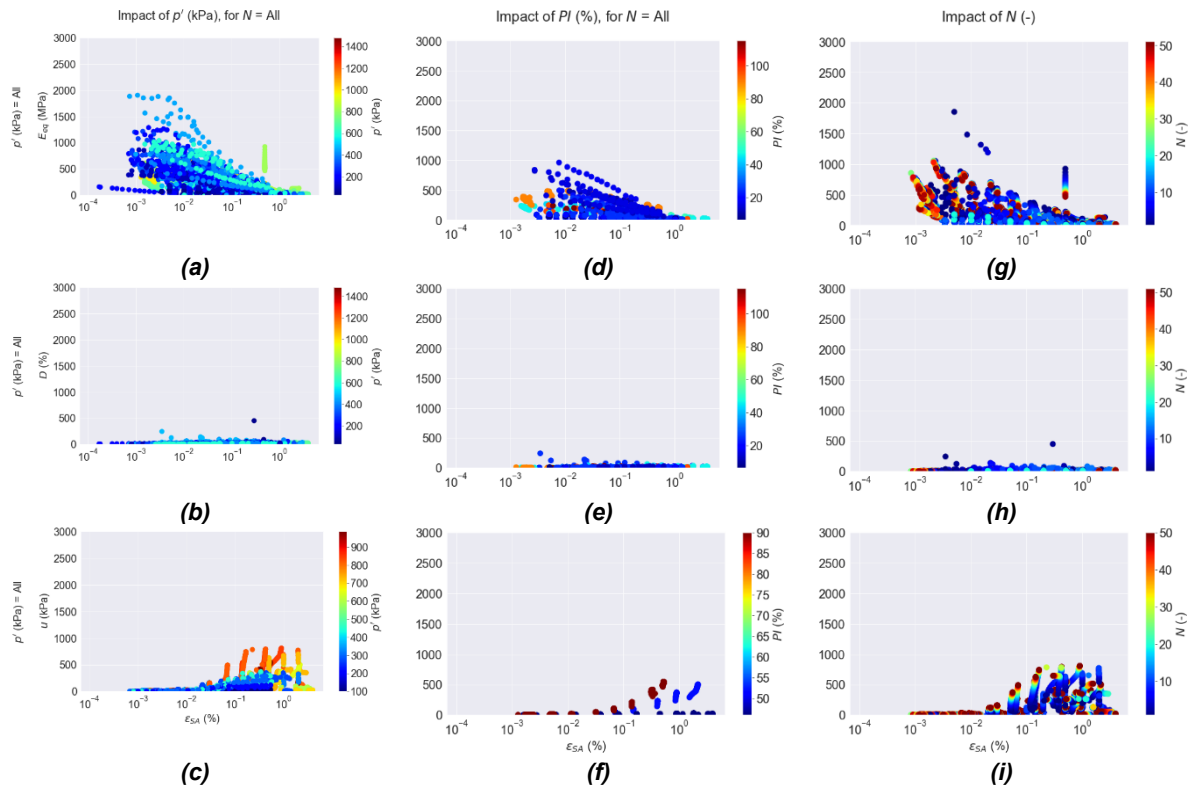


Figure 14 Cyclic triaxial tests: variation of equivalent axial modulus, damping ratio and pore water pressure with single amplitude axial strain according to mean effective confining pressure (a, b, c), to plasticity index (d, e, f) and number of cycle (g, h, i)

3.4.1.2 Cross-correlations

The distribution and the cross-correlations of the the axial strain (ϵ_{SA}), the equivalent axial modulus (E_{eq}), the damping (D), the pore water pressure (u), the confining pressure (p') and the plasticity index (PI) are illustrated on the Figure 15 to Figure 17 for small, medium and large strain values. The diagonal illustrates the distribution of each parameter.

For the lowest strain, the soils mostly behave linearly. Therefore, no clear tendency can be seen between the non-linear parameters and the axial strain. For the medium strain, the secant modulus become to decrease with increasing axial strain, but the variability is very high the coefficient of correlation is still low below 0.2 in absolute value.

A slight correlation appears between the pore water pressure generation and the damping. For the highest strain, the correlation between the secant modulus and the strain increases but stay below 0.3 in absolute value.

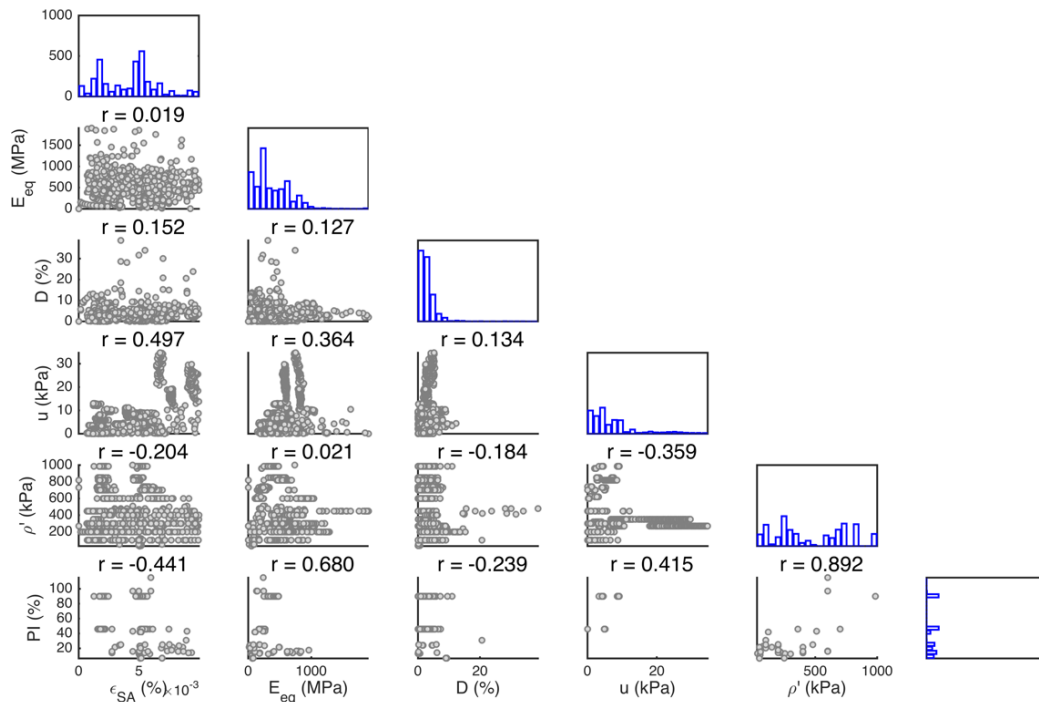


Figure 15 Correlations between ϵ_{SA} , E_{eq} , D , u , p' , PI for the cyclic triaxial tests. The values are given for single amplitude axial strain between 0.0001 till 0.01%

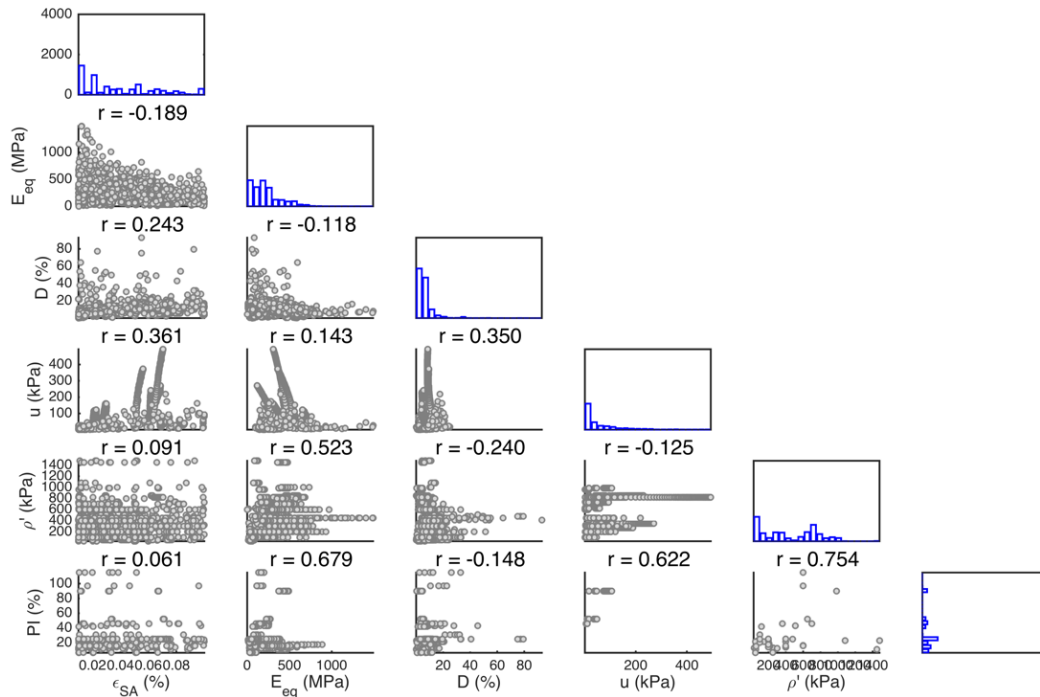


Figure 16 Correlations between ε_{SA} , E_{eq} , D , u , p' , PI for the cyclic triaxial tests. The values are given for single amplitude axial strain between 0.01 till 0.1%

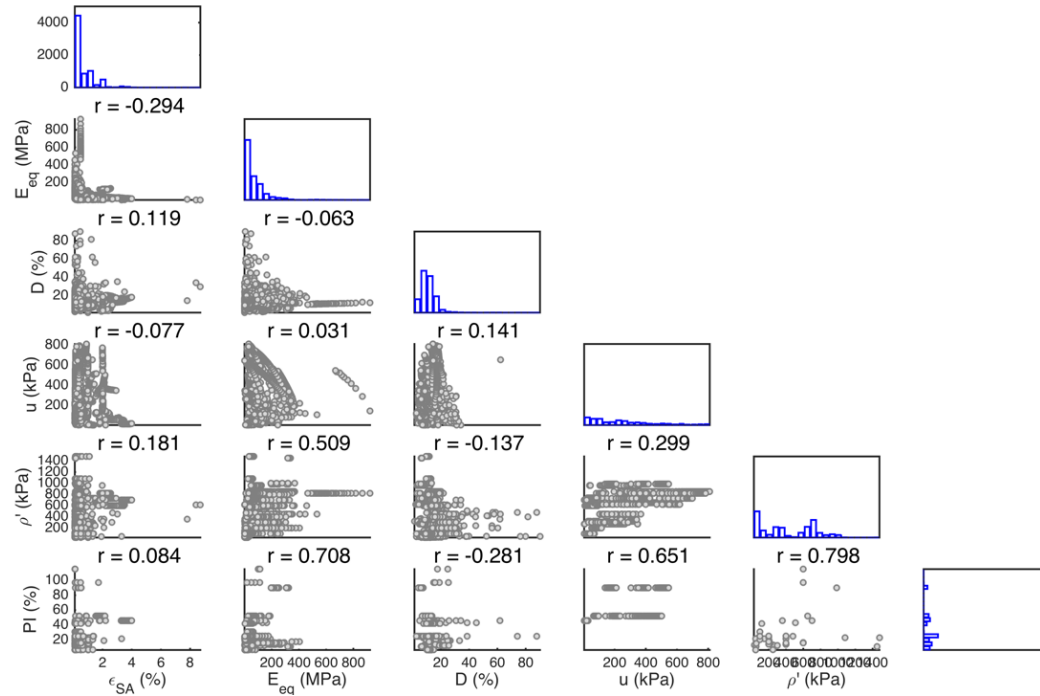


Figure 17 Correlations between ε_{SA} , E_{eq} , D , u , p' , PI for the cyclic triaxial tests. The values are given for single amplitude axial strain between 0.1 till 1%

3.4.1.3 Volumetric strain threshold

For the use and calibration of numerical models knowing the domain of validity of the calculations involving pore water pressure has capital importance. As tests were performed in non-drained conditions, we use water pressure data available as functions of the axial strain to calculate the volumetric strain threshold. This is here defined as the value of the axial strain at which the ratio of the pore water pressure respect to the confining pressure considered goes over 1% (Facciorusso, 2021). The volumetric strains are deduced for each number of cycle and for all the specimens (Figure 18).

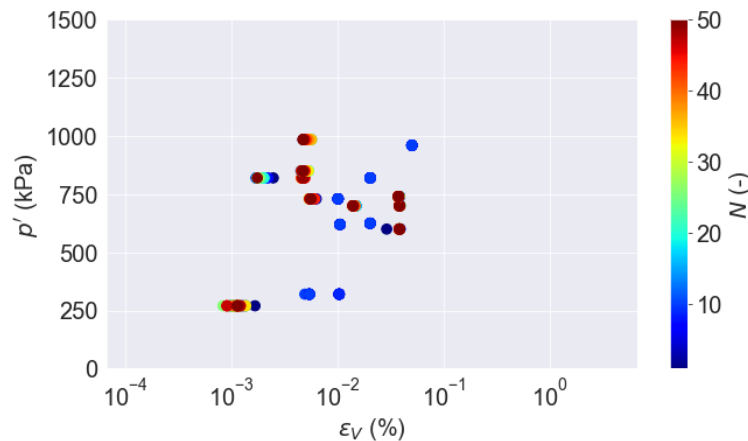


Figure 18 Volumetric strain threshold against the confining pressure. The color scale refers to the number of cycles of loading

3.4.2 Resonant Column tests

The following sections present : the evolution of the main dynamic soil properties, shear modulus, damping and pore water pressure according to the single amplitude shear strain (ϵ_{SA}) for the resonant column tests, cross-correlation and distributions of pertinent parameters for three single-amplitude shear strain intervals. To illustrate the influence of two parameters simultaneously on the dynamic soil properties, results are stored according to the mean effective confining pressure and another physical/laboratory parameter (soil type, plasticity index, or number of cycles), figures and comments are presented Appendix.

3.4.2.1 Dynamic properties

For the resonant column tests, we have two types of results. Most of the tests were performed with a torsional shear solicitation and rare tests were performed with an axial solicitation and will not be presented in the report. In the following figures, we will observe the influence of the mean effective confining pressure, PI and soil type on the same dynamic properties.

The influence of the soil type is illustrated on Figure 19. The down correlation lines are poorly constrained with very large variability especially of the equivalent shear modulus values. No clear tendency is observed.

The influence of the confining pressure is illustrated on Figure 20 (a, b and c). As for the cyclic triaxial tests, there is not a clear tendency. However, we can observe that for confining pressure above 1000 KPa, the equivalent shear modulus is above 400 MPa.

The influence of PI is illustrated on Figure 20 (d, e and f). On this limited dataset, no tendency is observed.

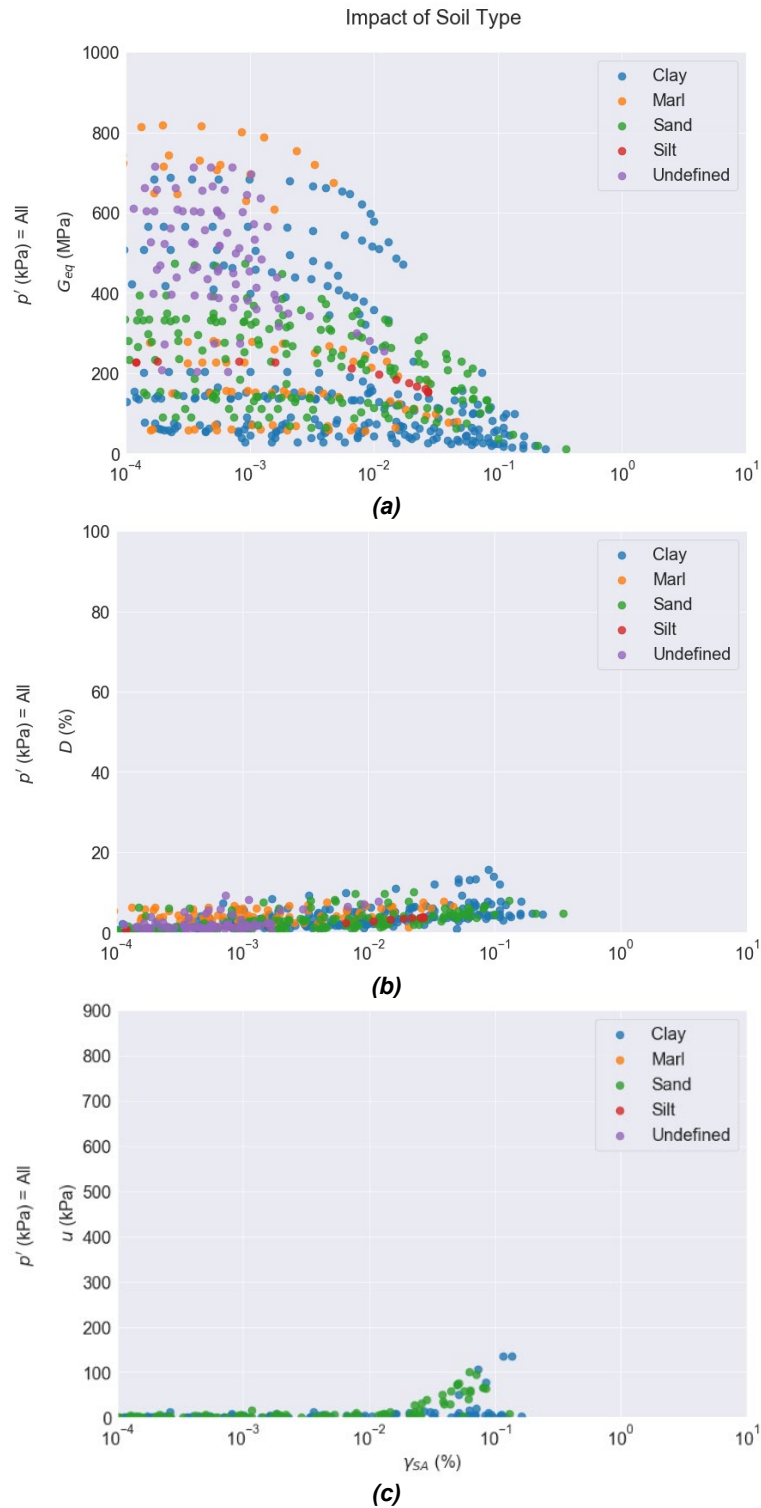


Figure 19 Resonant column tests; variation of equivalent shear modulus, damping and pore water pressure with single amplitude shear strain according to the soil type (a, b and c)

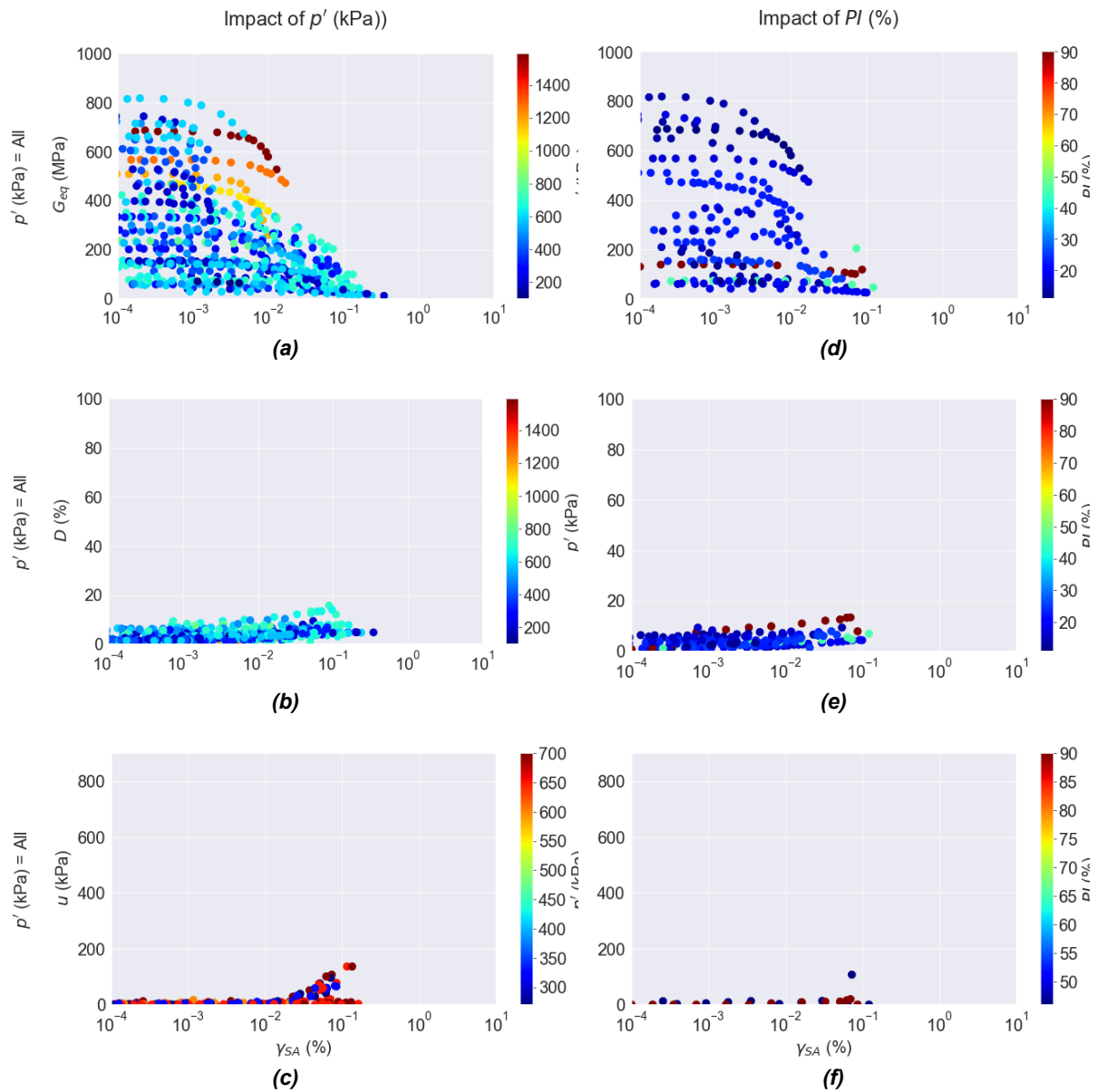


Figure 20 Resonant column tests; variation of evolution of the three main dynamic soil properties: shear modulus curves (G_{eq}), damping ratio (D) and pore pressure (u) curves with single amplitude shear strain (γ_{SA}) according to the confining pressure (a, b and c) and according to the plasticity index (d, e and f)

3.4.2.2 Cross-correlations

The distribution and the cross-correlations of the shear strain (γ_{SA}), the equivalent shear modulus (G_{eq}), the Damping (D), the confining pressure (p') and the plasticity index (PI) are illustrated on Figure 21 to Figure 23 for small, medium and large strain values. The diagonal illustrates the distribution of each parameter.

Similarly, to what was observed for the cyclic triaxial tests, for small strain no clear tendency can be seen between the shear strain and the non-linear parameters. The shear modulus has a significant correlation with the confining pressure. For medium strain, the correlations between the shear modulus, and the damping with strain increase as well as the correlation between the confining pressure and the shear modulus. A high correlation greater than 0.75, between the damping and the plasticity index, is observed. At high strain, few data is available and no tendency can be observed.

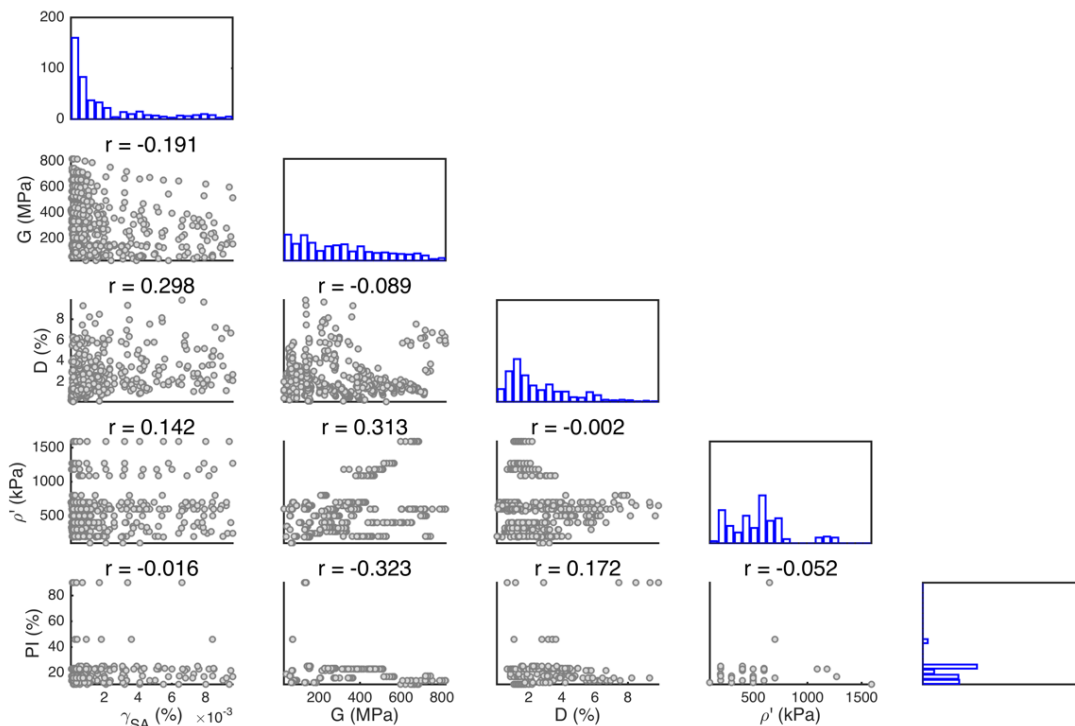


Figure 21 Correlations between γ_{SA} , G_{eq} , D , p' , PI for the resonant column tests. The values are given for single amplitude shear strain between 0.0001 till 0.01 %

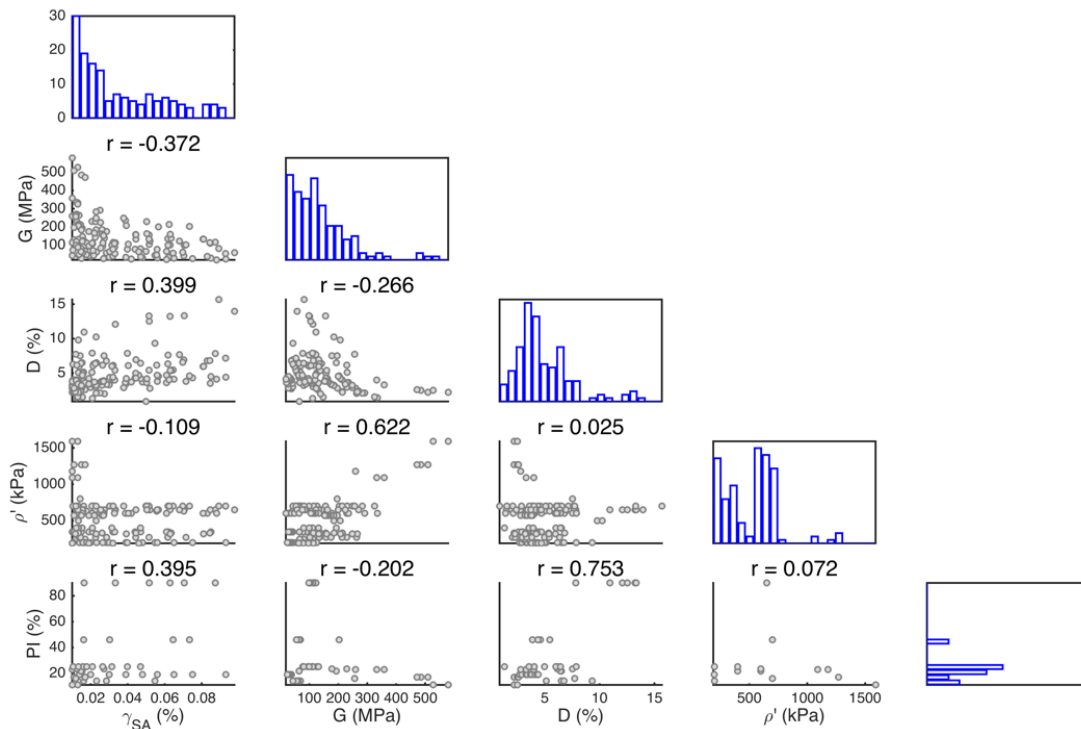


Figure 22 Correlations between γ_{SA} , G_{eq} , D , p' , PI for the resonant column tests. The values are given for single amplitude shear strain between 0.01 till 0.1 %

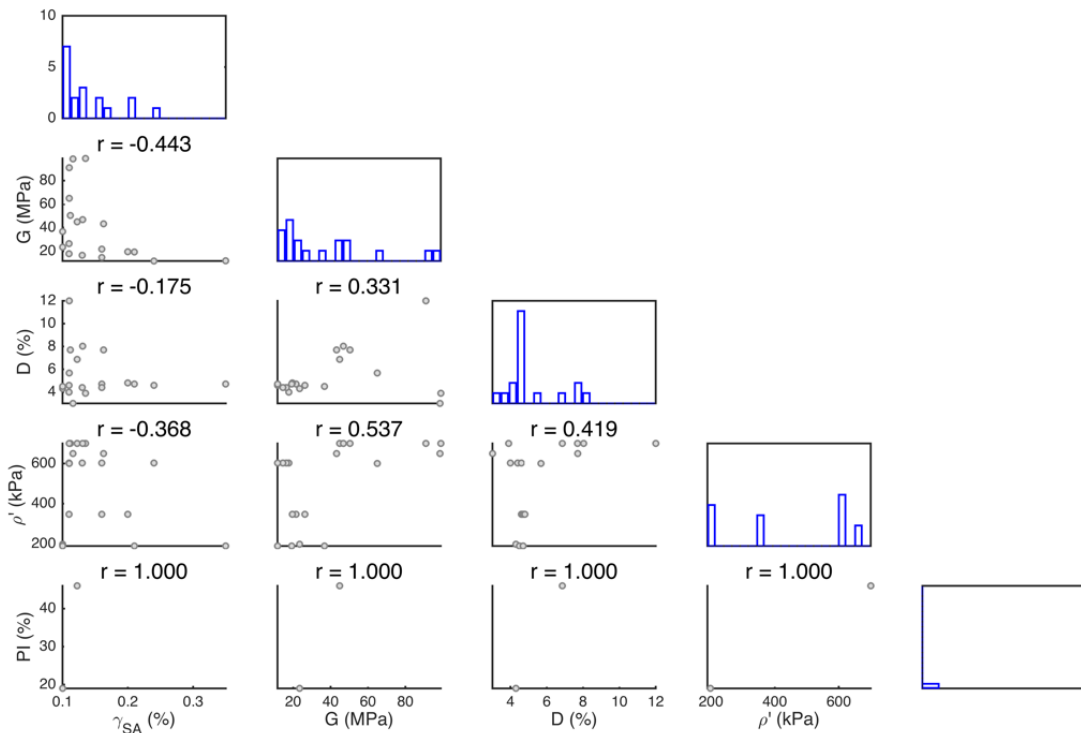


Figure 23 Correlations between γ_{SA} , G_{eq} , D , p' , PI for the resonant column tests. The values are given for single amplitude shear strain between 0.1 till 1 %

4 COMPARISON WITH INTERNATIONAL DATABASES

During our literature review, we selected three main databases to compare with the proposed databases which are the ones by Darendeli (2001), the Zhang et al. (2008) and Ciancimino et al. (2020). These three databases were chosen because, for each of them, a predictive model for the dynamic soil properties was deduced with the associated uncertainties. More in particular for these three databases we can assert what follows.

- The Darendeli (2001) database is a large database of 110 samples collected in the United States and Taiwan at 20 different sites. The database included the results of resonant column (RC) and torsional shear (TS) tests on soil specimens ranging from natural sands to clays, over a wide range of depth (3-263 m), mean effective confining pressure (230-2700 kPa), Plasticity Index PI (0-132) and over-consolidation ratio OCR (1-8). Based on a statistical analysis, the Author deduced analytical formulations for $G_{eq}/G_0 - \gamma_{SA}$ and $D - \gamma_{SA}$ curves. The most important parameters of the model are PI and the mean effective confining stress. When these last two parameters increase, $G_{eq}/G_0 - \gamma_{SA}$ curves move to the right (i.e. characterized by greater linear thresholds) and the curves $D - \gamma_{SA}$ move down (decreasing of the values for a given shear distortion). In the Darendeli's model, the effects of factors such as f , N and OCR are also taken into account. The model shows a narrower range of curves for varying values of PI compared to the database by Vucetic & Dobry (1991) and by Guerreiro et al. (2012). Bedr et al. (2019).
- The Zhang et al. (2008) database was developed based on a compilation of combined resonant column-torsional shear (TS/RC) test results performed on 122 natural samples of different geological ages. For the 122 samples, 8 are of Quaternary age, 66 are of Tertiary age and 48 come from residual soils and Saprolite deposits for which no specific deposition time has been given. The Authors proposed predictive equations to estimate $G_{eq}/G_0 - \gamma_{SA}$ and $D - \gamma_{SA}$ curves, with respect to PI , σ'_m or p' and the geological age.
- The Ciancimino et al. (2020) database consists of 79 samples investigated by means of dynamic resonant column tests, cyclic torsional shear tests and cyclic direct simple shear tests. Results are firstly analyzed highlighting the influence of the sample disturbance and of the mean effective consolidation pressure. The shear cyclic thresholds as a function of the plasticity index are then compared with values belonging to other published literature and differences were studied. Subsequently, the damping ratio is also investigated at small strains and differences between results from different tests are analyzed for various loading frequencies. Finally, the database is used to develop a predictive model for soil non-linear curves according to the plasticity index, mean effective confining stress and loading frequency. The model represents a useful tool to predict the non-linear stress-strain behaviour of Central Italy soils, necessary to perform site-specific ground response analyses.

The database called SIGMA2-WP4-2021 is hereafter compared with the three previous international databases. Figure 24 shows the comparison of the number of tested sites, the type of tests performed, the number of tests according to the type of soil, the plasticity index, the confining pressure and the depth of the collected soil specimens.

With its 69 studied sites, the Ciancimino et al. (2020) database contains the largest number of sites. However, few tests are available per site and only resonant column and cyclic shear tests were performed. The Darendeli (2001) and Zhang et al. (2008) databases are limited to resonant column tests with more than 100 tests.

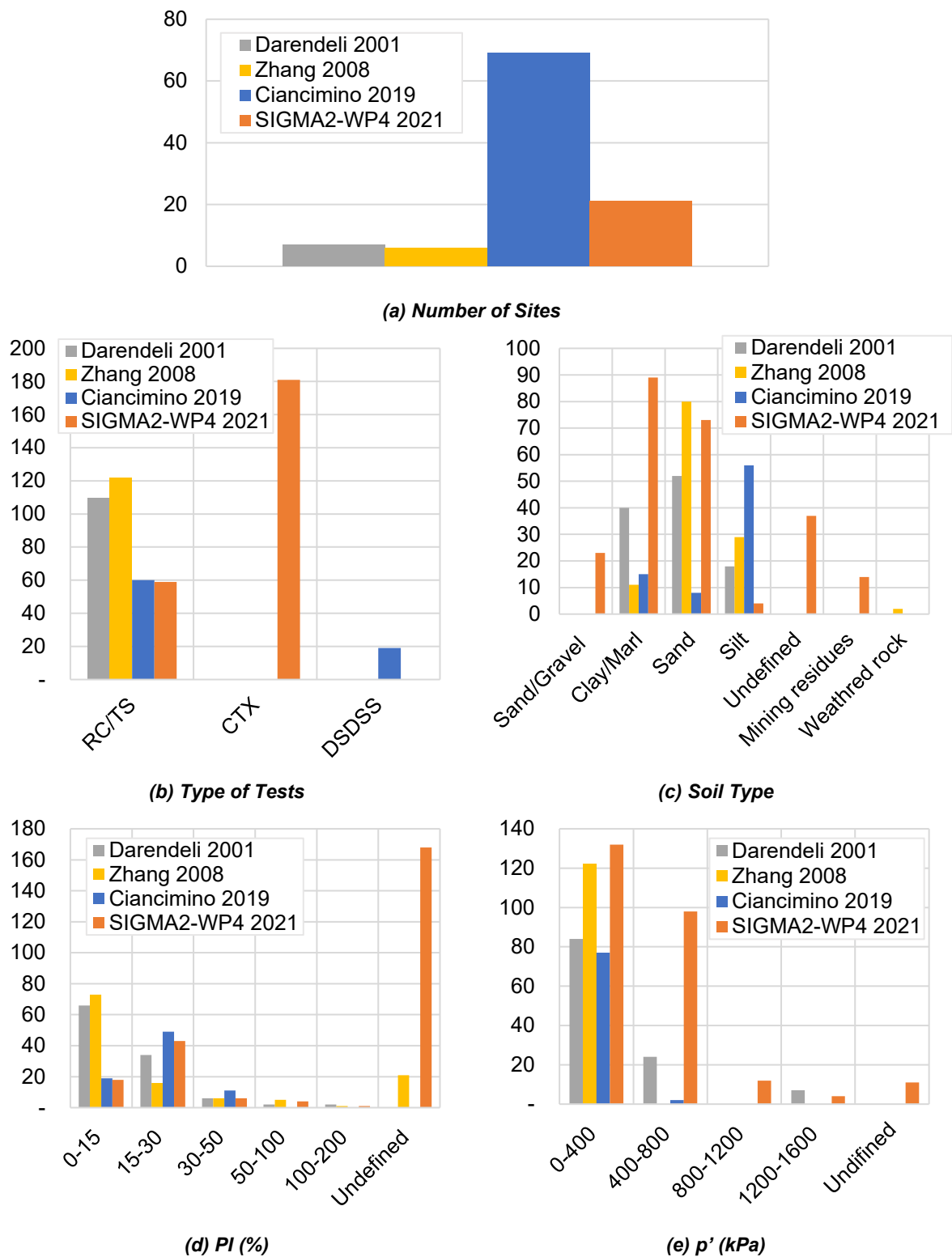


Figure 24 Comparison and discussion of the database proposed with the ones by Darendeli (2001) Zhang et al. (2008) and Ciancimino et al. (2020) : (a) Sites/Locations, (b) Tests type, (c) Soil types, (d) PI (%), (e) Mean effective confining pressure, p' (kPa)

	Research and Development Program On Seismic Ground Motion	SIGMA2-2021-D4-083
		Page 40/50

The French database contains 21 sites and could be expanded with additional projects when they will be available. Besides, additional data could come from other French institutes such as Univ. Gustave Eiffel, ENPC, etc. The French database contains more than 59 resonant columns tests and has collected more than 180 cyclic triaxial tests making this database the largest one in terms of tests performed. Besides, the combination of these two types of tests allows the definition of the dynamic soil properties from very low to large strains.

The French database contains the largest range of soils: mostly tests performed on sand (103), on clay (92), on sand and gravel (21), on mining residuals (17) and few on silt (3). For 37 samples, the lithological characterization is unknown, further investigations could lead to improvements of this type of metadata. The PI values are unknown in a large number of soil samples (168). In fact, usually, the geotechnical engineers perform plasticity test considering specimens cut from the same lithology but not exactly for the specimens after the accomplishment of the test in the cyclic devices. The French database includes tests performed for confining pressures until 1600 kPa, these data come from soil samples until 200m in depth.

5 CONCLUSIONS

This report is the referent document associated with the geotechnical database created using the results of the laboratory tests performed by the Cerema and EDF. The purpose of this report was to present the data collected and homogenized and also to indicate the structuration of the database and the first preliminary analysis of the collected data.

In total, 240 samples were collected, 59 from resonant column tests and 181 from cyclic triaxial tests. In total 21 sites were characterized. The data and the structuration of the database have been established to be consistent with the AGS format.

In comparison with three international geotechnical databases Ciancimino et al., (2020); Darendeli (2001) and Zhang et al. (2005), it represents the largest database in terms of the number of tests. Cyclic triaxial tests and resonant column tests are complementary to have a description of the cyclic soil behavior from very low to very high values of strain.

Besides, the here-proposed database has three main particularities containing: 1) measurements of dynamic soil properties at very high mean effective confining pressure (up to 1600 kPa); 2) measurements of alluvial (Sand/Gravel) soils with high particle size for which specific material and devices had to be considered; and 3) measurements of pore water pressures in combination with modulus and damping.

The first analysis of the database indicates correlations between the non-linear parameters and the strain but are low. It can be explained by the fact that the axial and shear modulus are not normalized at this stage. Correlation between the damping and the plasticity index is observed for the resonant column tests. For all tests a link between the confining pressure and the plasticity index is observed and is explained by the natural structuration of the soil layers for which the high plasticity index material is more likely to be located at depth.

The completeness of the database and the possibility to use jointly the Italian database Ciancimino et al. (2020) open plenty of perspectives concerning the improvement of the definition of the dynamic soil properties adapted to the French context.

The post-processing of data contained in the here defined database will consist in: 1) the normalization of equivalent axial modulus and pore water pressure curves, 2) converting single amplitude axial strain of *CTX* results to single amplitude shear strain to infer on shear modulus reduction curves, 3) interpreting data to deduce analytical relations between relevant parameters and dynamic curves, 4) define threshold shear strains, 4) analyzing and to quantifying uncertainties, and finally 5) propose predictive analytical models for dynamic soil properties with the associated uncertainties.

REFERENCES

- Anderson, D. G. (2003). *Laboratory Testing of Nonlinear Soil Properties: I & II*.
- Arkinsos, J. H., & Sallfors, G. (1991). Experimental determination of soil properties. *Proceedings of the 10th ECSMFE*, 3, 915–956.
- Bard, P.-Y., & Bouchon, M. (1985). The two-dimensional resonance of sediment-filled valleys. *Bulletin of the Seismological Society of America*, 75, 519–541.
- Bard, P.-Y., Campillo, M., Chavez-Garcia, F. J., & Sanchez-Sesma, F. (1988). The Mexico earthquake of September 19, 1985—A theoretical investigation of large-and small-scale amplification effects in the Mexico City Valley. *Earthquake Spectra*, 4(3), 609–633.
- Baroux, E., Pino, N. A., Valensise, G., Scotti, O., & Cushing, M. E. (2003). Source parameters of the 11 June 1909, Lambesc (Provence, southeastern France) earthquake: A reappraisal based on macroseismic, seismological, and geodetic observations. *Journal of Geophysical Research: Solid Earth*, 108(B9).
- Bedr, S., Mezouar, N., Verrucci, L., & Lanzo, G. (2019). Investigation on shear modulus and damping ratio of Algiers marls under cyclic and dynamic loading conditions. *Bulletin of Engineering Geology and the Environment*, 78(4), 2473–2493.
- Ciancimino, A., Lanzo, G., Alleanza, G. A., Amoroso, S., Bardotti, R., Biondi, G., Cascone, E., Castelli, F., Di Giulio, A., d’Onofrio, A., Foti, S., Lentini, V., Madiati, C., & Vessia, G. (2020a). Dynamic characterization of fine-grained soils in Central Italy by laboratory testing. *Bulletin of Earthquake Engineering*, 18(12), 5503–5531. <https://doi.org/10.1007/s10518-019-00611-6>
- Dammala, P. K., Kumar, S. S., Krishna, A. M., & Bhattacharya, S. (2019). Dynamic soil properties and liquefaction potential of northeast Indian soil for non-linear effective stress analysis. *Bulletin of Earthquake Engineering*, 17(6), 2899–2933. <https://doi.org/10.1007/s10518-019-00592-6>
- Darendeli, M. B. (2001). *Development of a new family of normalized modulus reduction and material damping curves*.
- Dobry, R., & Vucetic, M. (1987). *Dynamic properties and seismic response of soft clay deposits*.
- Electronic Transfer of Geotechnical and Geoenvironmental Data AGS4*. (2020). Association of Geotechnical and Geoenvironmental Specialists. <https://www.ags.org.uk/content/uploads/2020/12/AGS4-v-4.1-December-2020-1.pdf>
- Facciorusso, J. (2021). An archive of data from resonant column and cyclic torsional shear tests performed on Italian clays. *Earthquake Spectra*, 37(1), 545–562.
- Gobbi, S., Reiffsteck, P., Semblat, J. F., Lenti, L., & Santisi D’Avila, M. P. (2020a). *Liquefaction triggering in silty sands: Effects of non-plastic fines and mixture-packing conditions*.
- Guerreiro, P., Kontoe, S., & Taborda, D. (2012). Comparative study of stiffness reduction and damping curves. *15th World Conference on Earthquake Engineering, Lisbon, CD ROM*, 1–10.
- Hsu, C.-C. (2002). *Dynamic and cyclic behavior of soils over the wide range of shear strains in NGI-type simple shear testing devices*. University of California, Los Angeles.

	Research and Development Program On Seismic Ground Motion	SIGMA2-2021-D4-083
		Page 43/50

Ishibashi, I., & Zhang, X. (1993). Unified Dynamic shear moduli and damping ratio of sand and clay. *Soils and Foundations*, 33, 182–191.

Ishihara, K. (1996). *Soil Behaviour in Earthquake Geotechnics*. Clarenton Press.

Kishida, T. (2017). Comparison and correction of modulus reduction models for clays and silts. *Journal of Geotechnical and Geoenvironmental Engineering*, 143(4), 04016110.

Kumar, S. S., Krishna, A. M., & Dey, A. (2017). Evaluation of dynamic properties of sandy soil at high cyclic strains. *Soil Dynamics and Earthquake Engineering*, 99, 157–167.

Lanzo, G., & Vucetic, M. (1999a). Effect of soil plasticity on damping ratio at small cyclic strains. *Soils and Foundations*, 39(4), 131–141.

Larroque, C., Scotti, O., & Ioualalen, M. (2012). Reappraisal of the 1887 Ligurian earthquake (western Mediterranean) from macroseismicity, active tectonics and tsunami modelling. *Geophysical Journal International*, 190(1), 87–104. <https://doi.org/10.1111/j.1365-246X.2012.05498.x>

Lenti, L. (2017). *HDR Evaluation des mouvements du sol sous sollicitations sismiques et vibratoires*. Université Paris-Est.

Lo Presti, D. C. F., & O'Neill, D. A. (1991). Laboratory investigation of small strain modulus anisotropy in sands. *Proc. ISOCCTI, Clarkson University, Potsdam*, 213–224.

Mair, R. J. (1993). Unwin memorial lecture 1992. Developpements in geotechnical engineering research: Application to tunnels and deep excavation. *Proceedings of the Institution of Civil Engineers-Civil Engineering*, 97(1), 27–41.

Matesic, L., Hsu, C.-C., D'Elia, M., & Vucetic, M. (2010). *Development of Database of Cyclic Soil Properties from 94 Tests on 47 Soils*.

Menq, F. (2003). *Dynamic properties of sandy and gravelly soils*.

Mori, H., & Tsuchiya, H. (1981). *In Situ Measurement on Dynamic Modulus and Damping of Pleistocene Soils*. 5.

Mortezaie, A., & Vucetic, M. (2016). Threshold shear strains for cyclic degradation and cyclic pore water pressure generation in two clays. *Journal of Geotechnical and Geoenvironmental Engineering*, 142(5), 04016007.

Pagliaroli, A. (2018). Key issues in Seismic Microzonation studies: Lessons from recent experiences in Italy. *Rivista Italiana Di Geotecnica*, 1(1), 5–48.

Park, D., & Kishida, T. (2019). Shear modulus reduction and damping ratio curves for earth core materials of dams. *Canadian Geotechnical Journal*, 56(1), 14–22.

Pyke, R., Laird, J., & North, J. (2007). *EVALUATION OF UNCERTAINTIES IN DYNAMIC PROPERTIES*. 1359.

Régnier, J., Bonilla, L.-F., Bard, P.-Y., Bertrand, E., Hollender, F., Kawase, H., Sicilia, D., Arduino, P., Amorosi, A., & Asimaki, D. (2018). PRENOLIN: International Benchmark on 1D Nonlinear Site-Response Analysis—Validation Phase Exercise. *Bulletin of the Seismological Society of America*.

Régnier, J., Cadet, H., Bonilla, L. F., Bertrand, E., & Semblat, J.-F. (2013). Assessing Nonlinear Behavior of Soils in Seismic Site Response: Statistical Analysis on KiK-net Strong-Motion Data. *Bulletin of the Seismological Society of America*, 103(3), 1750–1770.

	Research and Development Program On Seismic Ground Motion	SIGMA2-2021-D4-083
		Page 44/50

Ritz, J.-F., Baize, S., Ferry, M., Larroque, C., Audin, L., Delouis, B., & Mathot, E. (2020). Surface rupture and shallow fault reactivation during the 2019 Mw 4.9 Le Teil earthquake, France. *Communications Earth & Environment*, 1(1), 10. <https://doi.org/10.1038/s43247-020-0012-z>

Rohatgi, A. (2021). *Webplotdigitizer* (4.5) [Computer software]. <https://automeris.io/WebPlotDigitizer>

Seed, H. B., & Idriss, I. M. (1971). Simplified procedure for evaluating soil liquefaction potential. *Journal of Soil Mechanics & Foundations Div.*

Serratrice, J.-F. (2016). Mesures des propriétés cycliques des sols limoneux ou argileux au laboratoire. *Revue Française de Géotechnique*, 148, 1. <https://doi.org/10.1051/geotech/2016009>

Tabata, K., & Vucetic, M. (2010). *Threshold shear strain for cyclic degradation of three clays*.

Vucetic, M. (1994). Cyclic threshold shear strains in soils. *Journal of Geotechnical Engineering*, 120(12), 2208–2228.

Vucetic, M., & Dobry, R. (1991). Effect of soil plasticity on cyclic response. *Journal of Geotechnical Engineering*, 117(1).

Yoshida, N. (2015a). *Seismic ground response analysis*. Springer.

Zhang, J., Andrus, R. D., & Juang, C. H. (2005). Normalized shear modulus and material damping ratio relationships. *Journal of Geotechnical and Geoenvironmental Engineering*, 131(4), 453–464.

Zhang, J., Andrus, R. D., & Juang, C. H. (2008a). Model uncertainty in normalized shear modulus and damping relationships. *Journal of Geotechnical and Geoenvironmental Engineering*, 134(1), 24–36.

APPENDIX : DYNAMIC SOIL PROPERTIES BY RANGE OF CONFINING PRESSURE

The following sections illustrate the content of database for different ranges of effective confining pressure pressures.

CYCLIC TRIAXIAL TESTS

Figure 25, Figure 26 and Figure 27 illustrate the variation of equivalent axial modulus, damping ratio and pore water pressure with the single amplitude axial strain according to the soil type (a, b, c and d) the PI (e, f, g and h) for a fixed number of cycle ($N=5$) and the number of cycles (i, j, k and l) for four ranges of effective confining pressure pressures.

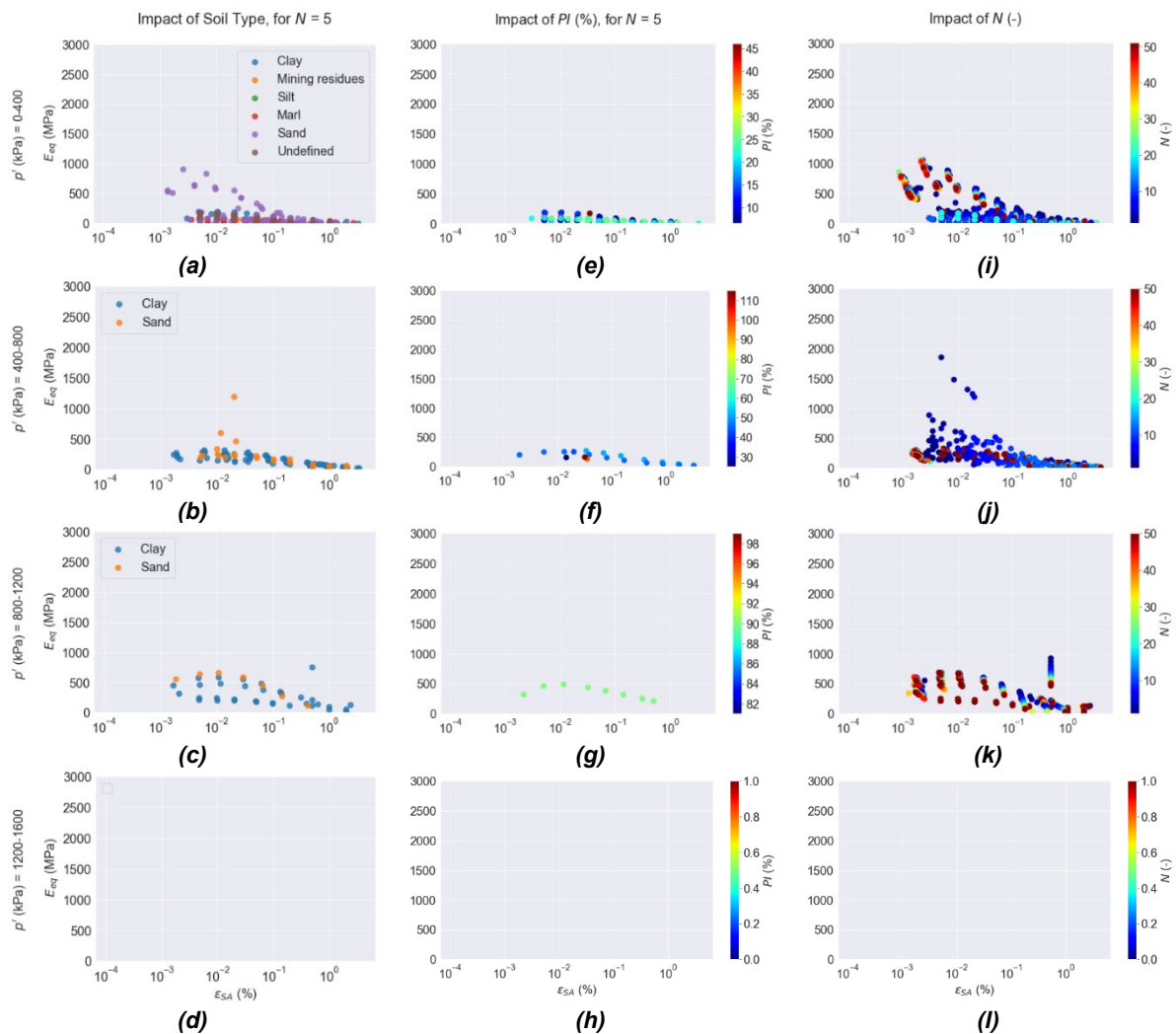


Figure 25 Cyclic triaxial tests; Young modulus curves versus the axial strain according to the soil type for different confining pressure ranges and for a number of cycles $N=5$ (a, b, c and d), according to the Plasticity Index for different confining pressure ranges and for a number of cycles $N=5$ (e, f, g and h), and according to the number of cycles for different confining pressure ranges (i, j, k and l)

The amount of data in each confining pressure range decrease as the confining pressure increase. No clear tendency appears between the equivalent axial modulus or the damping curves and the soil type or PI for a given confining pressure. The impact of the number of cycles is similar to what was observed with all data mixed that is a decrease of the equivalent axial modulus and a decrease of the damping with increasing N . According to Figure 27, the pore water pressure is higher for sand materials whatever the confining pressure regarded.

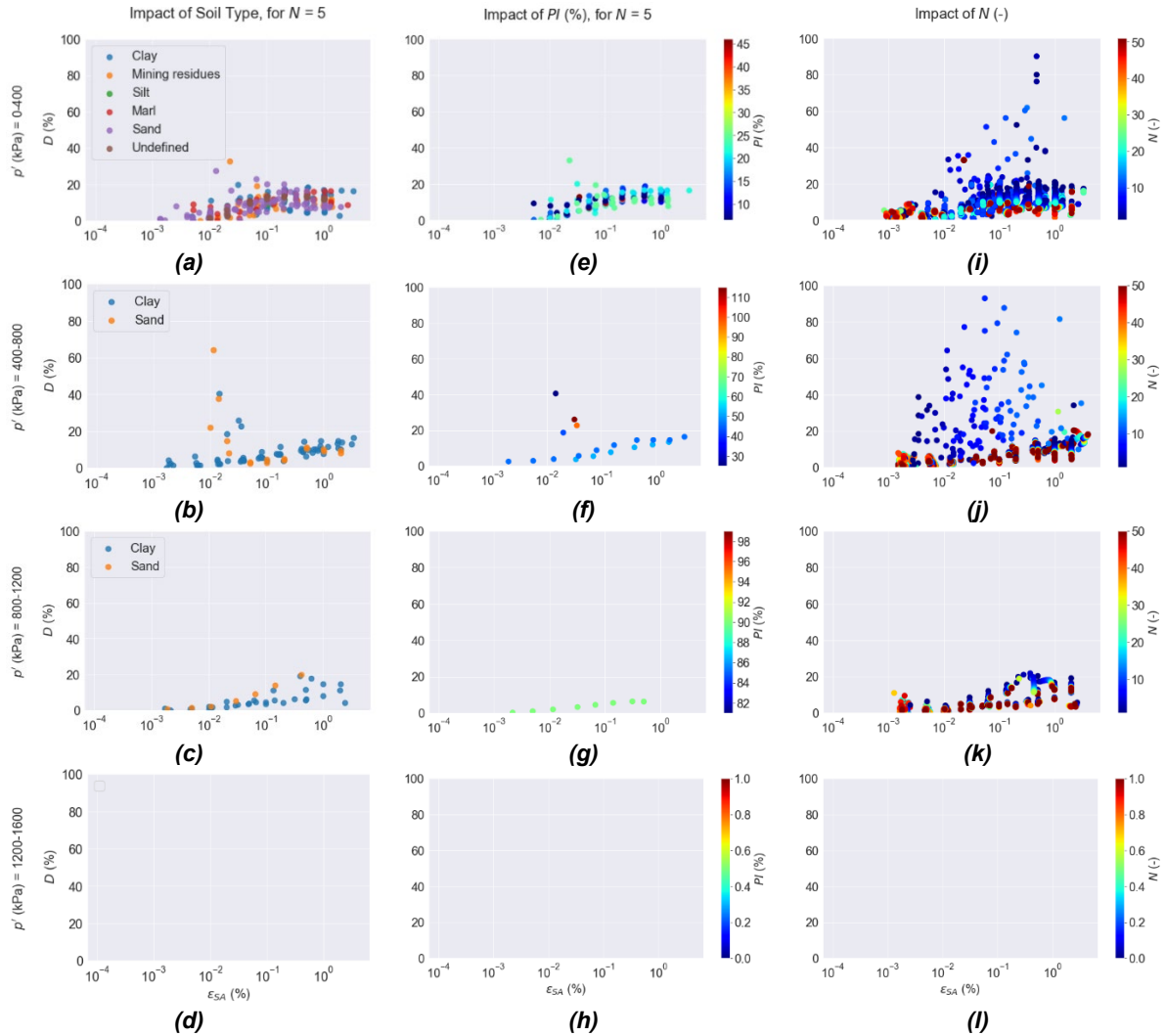


Figure 26 Cyclic triaxial tests: evolution of the Damping curves with axial strain according to the soil type for different confining pressure ranges and for a number of cycles $N=5$ (a, b, c and d) according to the Plasticity Index for different confining pressure ranges and for a number of cycles $N=5$ (e, f, g and h) and according to the number of cycles for different confining pressure ranges (i, j, k and l)

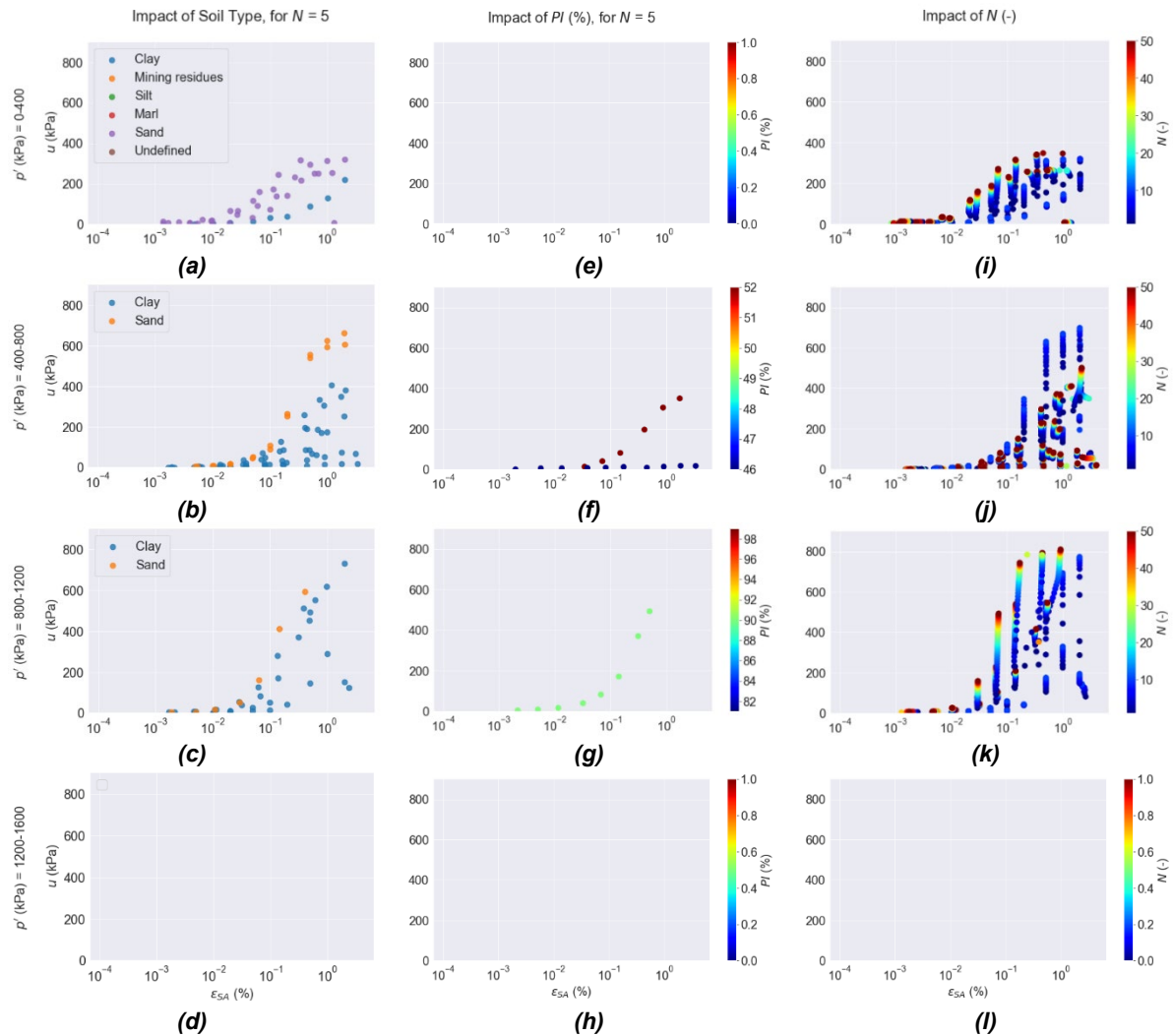


Figure 27 Cyclic triaxial tests: evolution of the pore water pressure curves with axial strain according to the soil type for different confining pressure ranges and for a number of cycles $N=5$ (a, b, c and d) according to the Plasticity Index for different confining pressure ranges and for a number of cycles $N=5$ (e, f, g and h) and according to the number of cycles for different confining pressure ranges (i, j, k and l)

RESONANT COLUMN TESTS

Figure 22, Figure 23 and Figure 30 illustrate the equivalent shear modulus, damping and pore water pressure variation with the single amplitude shear strain obtained from resonant column tests according to the soil type (a, b, c and d) and the plasticity Index (e, f, g and h) for four ranges of mean effective confining pressures.

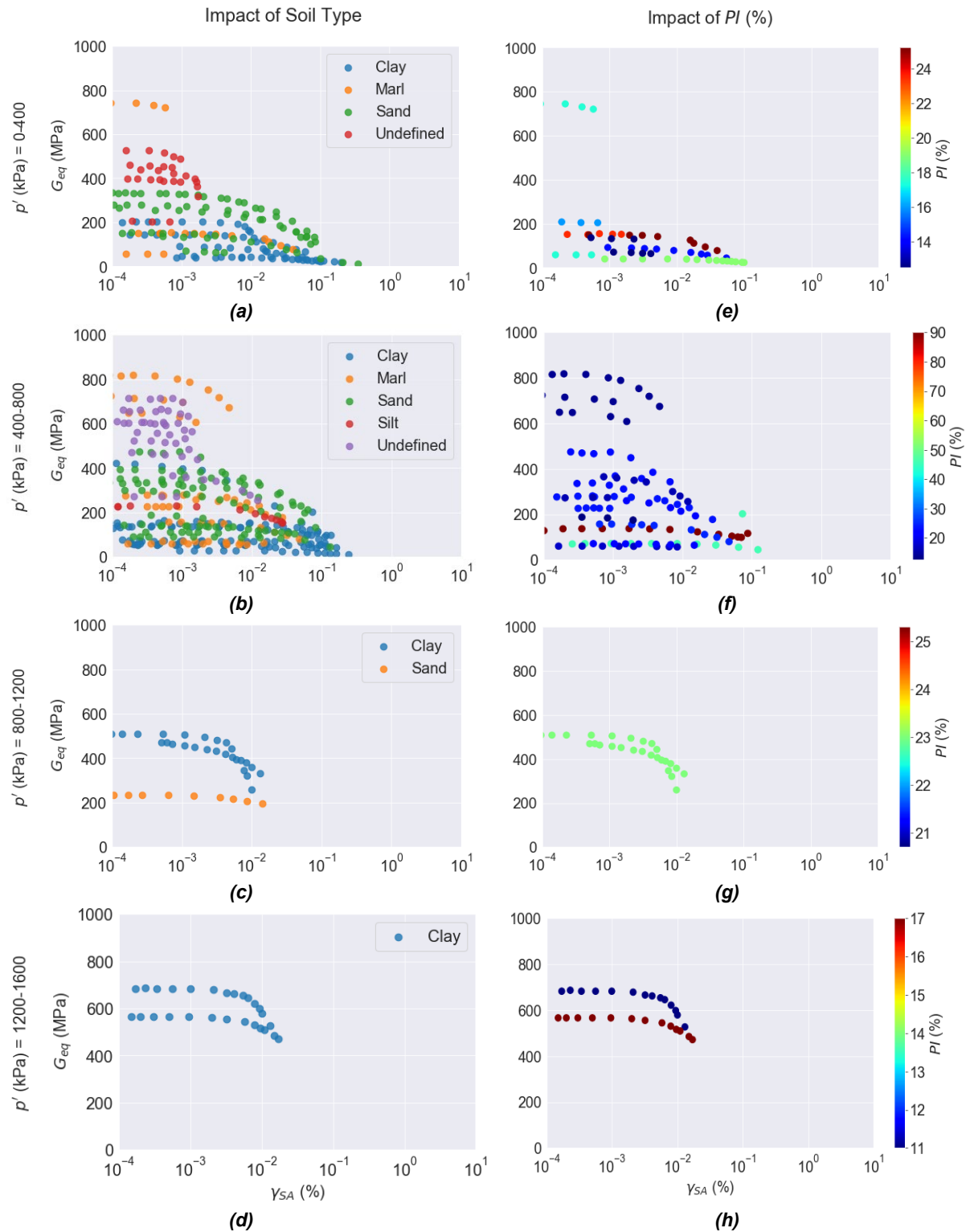


Figure 28 Resonant column tests; evolution of the shear modulus curves with distortion according to the soil type (a, b, c and d) and according to the Plasticity Index for different confining pressure ranges (e, f, g and h)

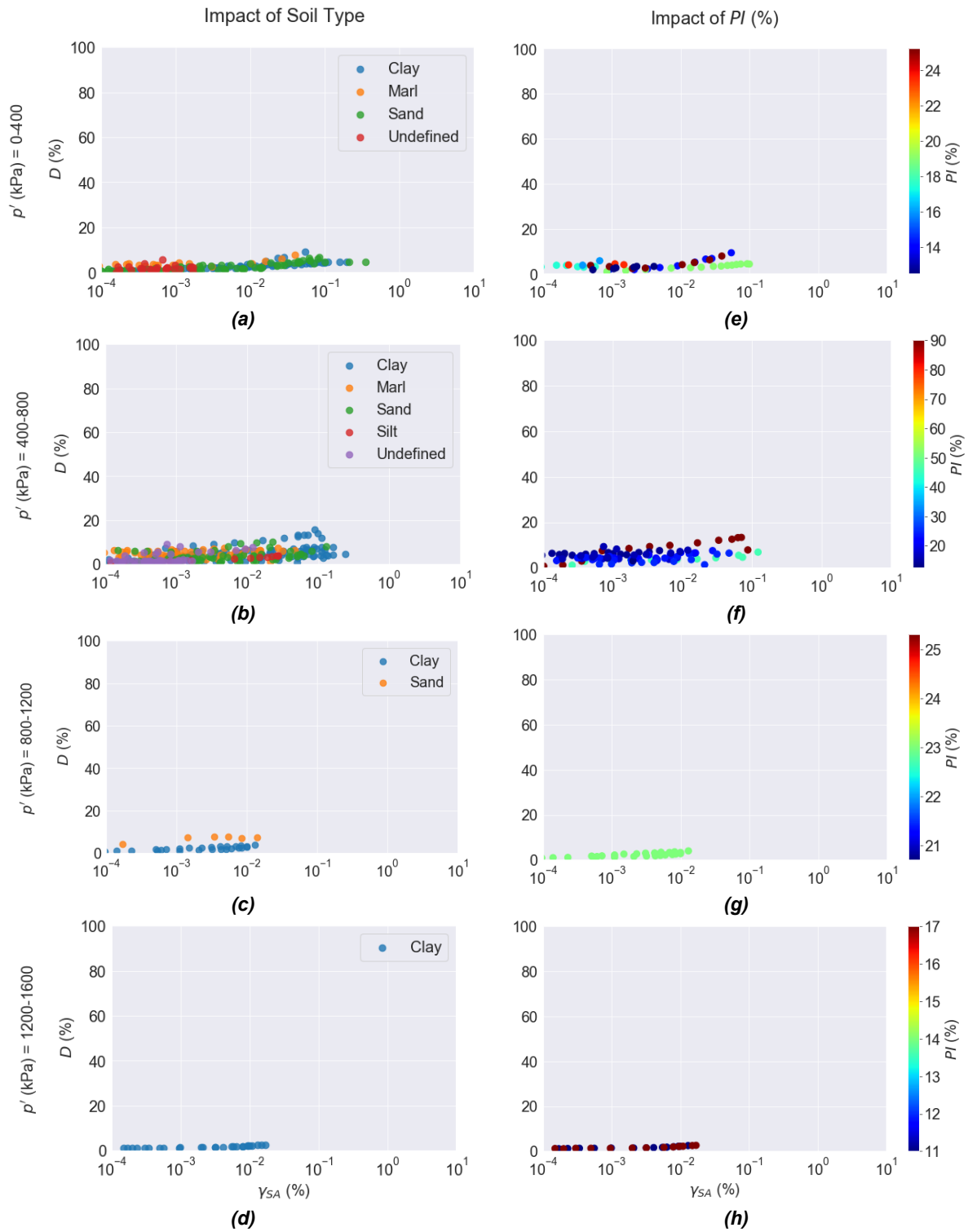


Figure 29 Resonant column tests; evolution of the shear modulus curves with distortion according to the soil type (a, b, c and d) and according to the Plasticity Index (e, f, g and h) and for different confining pressure ranges

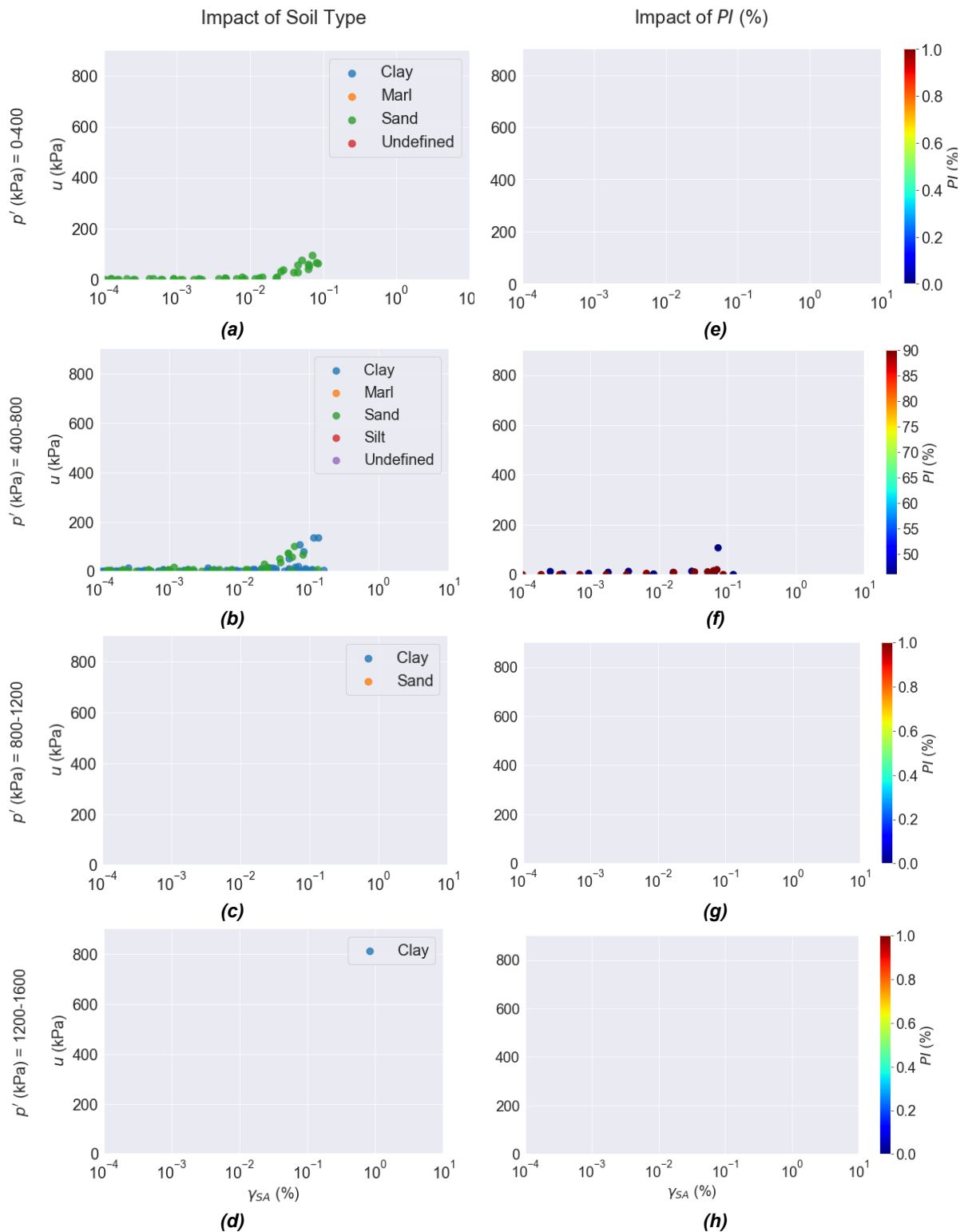


Figure 30 Resonant column tests; evolution of the pore water pressure curves with distortion according to the soil type (a, b, c and d) and according to the Plasticity Index (e, f, g and h) and for different confining pressure ranges